

**DERIVATION OF THE BOLTZMANN EQUATION  
FROM HARD-SPHERE DYNAMICS**  
[after Y. Deng, Z. Hani, and X. Ma]

by Thierry Bodineau, Isabelle Gallagher,  
Laure Saint-Raymond & Sergio Simonella

**Contents**

<a href="#">Introduction</a> .....	1
<a href="#">1. The Boltzmann equation</a> .....	3
<a href="#">2. Short time derivation</a> .....	7
<a href="#">3. Proof of Lanford's theorem using cluster expansions</a> .....	12
<a href="#">4. Long time derivation</a> .....	22
<a href="#">5. Consequences and perspectives</a> .....	34
<a href="#">References</a> .....	35

## Introduction

The Boltzmann equation describes the time evolution of the particle density of a collisional rarefied gas in the position and velocity phase space. Its success, together with the kinetic theory it gave rise to, represents an undisputed achievement in physics.

In this note we present the result by Deng, Hani, and Ma (2024), who derive the Boltzmann equation starting from a microscopic system of hard spheres, for times much larger than the mean free time (the average time between two collisions of a given particle): the derivation holds on the same time interval on which there is a smooth solution of the Boltzmann equation.

Let us start by describing the main theorem informally. A precise statement requires a number of definitions and will appear on page 23 (Theorem 4.1). Consider  $N$  hard spheres moving in  $\mathbb{R}^d$ , initially “independent” and identically distributed according to a distribution  $f^0 = f^0(x, v)$ . Assume that the Boltzmann equation with initial data  $f^0$  admits a smooth solution  $f$  on a time-span  $[0, T]$ . Then, for any  $t \in [0, T]$ , the (random) fraction of hard spheres in any set  $\Delta \subset \mathbb{R}^{2d}$  converges in probability to  $\int_{\Delta} f(t)$ , in the limit when the number of particles  $N \rightarrow \infty$  and their diameter  $\varepsilon \rightarrow 0$  in such a way that the mean free time is of order 1.

The problem of deriving the Boltzmann equation from microscopic systems has been addressed by many authors in the past century. An initial key step is the enlightening

work of Grad (1958) on the low-density scaling, where he wrote down an effective differential equation for the first correlation function in the low-density regime. The first mathematical result on this problem goes back to Cercignani (1972) and to the celebrated theorem of Lanford (1975), who proved that in the special case of the hard-sphere system, the asymptotic factorisation of the correlation functions (known in kinetic theory as the *propagation of chaos* property) can be established by a careful study of trajectories. In particular, Lanford demonstrated that there is no contradiction between the reversibility in the microscopic laws of mechanics and the irreversibility exhibited by Boltzmann's equation. The proof was an important breakthrough and after a number of subsequent works until the early 2000's, the details of the argument were completed and the result refined and generalized<sup>(1)</sup>. The main limitation of the method — unsurpassed until the work of Deng, Hani and Ma except for some specific settings<sup>(2)</sup> — is that the result is only valid for a very short time: essentially a small fraction of the mean free time<sup>(3)</sup>. The reason for this drawback is that the method of proof consists in expanding the correlation functions into time series, which only converge for short times. Actually, the Boltzmann equation is itself very difficult to study mathematically and the existence and uniqueness of solutions for long times is only known in specific settings. This lack of stability is due to the locality of the interaction, which is also one of the reasons why it is so difficult to prove the convergence of the microscopic dynamics.

Deng, Hani and Ma were able, fifty years after the seminal paper by Lanford, to go beyond the short time restriction and to prove the long-awaited result that the convergence of the hard-sphere dynamics holds up to any time for which the Boltzmann equation has a smooth solution. Important ideas for this proof have already been devised in the series of works by Deng and Hani (2023a, 2026, 2023b) to derive a kinetic equation in the context of wave turbulence on long times (see Remark 4.4 for some comments).

In this paper, we present some of the key ideas of the proof of Deng, Hani, and Ma (2024). In Section 1 we introduce the Boltzmann equation and present some classical well-posedness results and their limitations. Section 2 is devoted to the presentation of the short time derivation result by Lanford (Theorem 2.1). A pictorial sketch of proof of Lanford's theorem is provided in Section 3: this somewhat unusual presentation is designed as a preparation to the presentation of the proof of the theorem by Deng, Hani

<sup>(1)</sup>See Spohn (1991), Cercignani, Illner, and Pulvirenti (1994), Cercignani, Gerasimenko, and Petrina (1997), Matthies and Theil (2012) Gallagher, Saint-Raymond, and Texier (2014), Pulvirenti, Saffirio, and Simonella (2014), Ayi (2017), Gerasimenko and Gapyak (2021), Le Bihan (2022), Dolmaire (2023).

<sup>(2)</sup>Perturbation of vacuum in (Illner and Pulvirenti, 1989; Denlinger, 2018), tagged particle at equilibrium in (van Beijeren, Lanford, Lebowitz, and Spohn, 1980; Bodineau, Gallagher, and Saint-Raymond, 2016; Catapano, 2018; Fougères, 2024) or fluctuations around equilibrium in (Bodineau, Gallagher, Saint-Raymond, and Simonella, 2023a, 2024b; Le Bihan, 2025a,b).

<sup>(3)</sup>To keep in mind the order of physical magnitudes, for a gas at room temperature and atmospheric pressure the mean free time is of the order of  $10^{-9}$  seconds, while the mean free path is of the order of  $10^{-5}$  meters.

and Ma (Theorem 4.1), which is provided in Section 4. Some consequences of the result, and perspectives, are given in Section 5.

*Acknowledgements.* — We are very grateful to François Golse, Mario Pulvirenti, Herbert Spohn and Isabelle Tristani for useful comments on a previous version of this manuscript. We especially thank Nicolas Bourbaki for a very thorough reading and many suggestions.

## 1. The Boltzmann equation

The Boltzmann equation, devised by Boltzmann in 1872, is the cornerstone of kinetic theory. It provides a statistical description of a gas constituted of identical particles moving in the  $d$ -dimensional space  $\mathbb{R}^d$  ( $d = 2, 3$ ) with uniform rectilinear motion between each elastic binary collision (see Section 2.1 below for more).

Under the assumption that the particles are independent and identically distributed (this is referred to as the “chaos assumption”), their common distribution  $f$  is expected to be a real-valued function depending on  $t \in \mathbb{R}$  (time),  $x \in \mathbb{R}^d$  (position) and  $v \in \mathbb{R}^d$  (velocity) satisfying the Boltzmann equation

$$(1) \quad \left\{ \begin{array}{l} \underbrace{\partial_t f(t, x, v) + v \cdot \nabla_x f(t, x, v)}_{\text{transport}} = \int_{\mathbb{R}^d \times \mathbb{S}^{d-1}} \left( \underbrace{f(t, x, v'_*) f(t, x, v')}_{\text{gain term}} - \underbrace{f(t, x, v_*) f(t, x, v)}_{\text{loss term}} \right) \\ \times \left( (v - v_*) \cdot \omega \right)_+ dv_* d\omega, \\ f(0, x, v) = f^0(x, v) \end{array} \right.$$

where the “pre-collisional” velocities  $(v', v'_*)$  in the “gain” term on the right-hand side are defined by the scattering laws

$$(2) \quad v' := v - \left( (v - v_*) \cdot \omega \right) \omega, \quad v'_* := v_* + \left( (v - v_*) \cdot \omega \right) \omega.$$

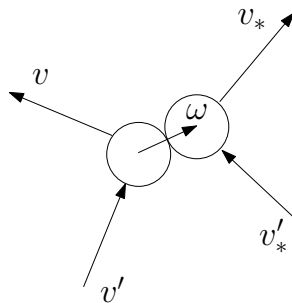


FIGURE 1. The hard-sphere scattering law.

Note that

$$(3) \quad \begin{aligned} v + v_* &= v' + v'_*, \\ |v|^2 + |v_*|^2 &= |v'|^2 + |v'_*|^2, \end{aligned}$$

which express the fact that collisions are elastic and thus momentum and energy are conserved during collisions. The initial value of  $f$  is prescribed to be a given function  $f^0$ . We have used the notation  $a_+$  for  $\max(0, a)$ .

In the following we shall use the shorthand notation

$$f_\star := f(v_\star), \quad f' := f(v') \quad \text{and} \quad f'_\star := f(v'_\star),$$

so that the right-hand side of (1) becomes

$$(4) \quad Q(f, f)(v) := \int (f' f'_\star - f f'_\star) ((v - v_\star) \cdot \omega)_+ dv_\star d\omega.$$

### 1.1. Conservation laws and H-Theorem

From (3) and using the well-known fact (see for instance Cercignani, 1972) that the mappings  $(v, v_\star) \mapsto (v_\star, v)$  and  $(v, v_\star, \omega) \mapsto (v', v'_\star, \omega)$  have unit Jacobian determinants, one can show formally that for any test function  $\varphi$  defined on  $\mathbb{R}^d$ , and with the notation introduced at the end of the previous paragraph,

$$\int Q(f, f) \varphi dv = \frac{1}{4} \int [f' f'_\star - f f'_\star] (\varphi + \varphi_\star - \varphi' - \varphi'_\star) ((v - v_\star) \cdot \omega)_+ dv dv_\star d\omega.$$

In particular, it can be shown that

$$\int Q(f, f) \varphi dv = 0 \quad \text{for all } f \text{ regular enough}$$

if and only if  $\varphi(v)$  is a collision invariant, meaning that  $\varphi(v)$  is a linear combination of  $\{1, v^1, \dots, v^d, |v|^2\}$ . Thus, successively multiplying the Boltzmann equation (1) by the collision invariants and then integrating in velocity gives rise formally to the *local conservation laws*:

$$\begin{aligned} \partial_t \int f(t, x, v) dv + \nabla_x \cdot \int f(t, x, v) v dv &= 0; \\ \partial_t \int f(t, x, v) v dv + \nabla_x \cdot \int f(t, x, v) v \otimes v dv &= 0; \\ \partial_t \int f(t, x, v) \frac{|v|^2}{2} dv + \nabla_x \cdot \int f(t, x, v) \frac{|v|^2}{2} v dv &= 0. \end{aligned}$$

The second line should be understood component-wise as

$$\forall 1 \leq i \leq d, \quad \partial_t \int f(t, x, v) v^i dv + \sum_{j=1}^d \partial_j \int f(t, x, v) v^i v^j dv = 0.$$

Taking  $\varphi = \log f$  and using the additivity of the logarithm shows that the collision operator is *dissipative* in the sense that

$$D(f) := - \int Q(f, f) \log f dx dv \geq 0$$

with equality if and only if  $\log f$  is a collision invariant. This leads to the entropy inequality

$$(5) \quad \int f \log f(t, x, v) dx dv + \int_0^t D(f)(s) ds \leq \int f^0 \log f^0(x, v) dx dv,$$

known since Boltzmann as the H-Theorem. Note that this increase in the entropy, defined by  $\int -f \log f(t, x, v) dx dv$  (which is strict unless  $f$  is an equilibrium, i.e. a spatially homogeneous Gaussian distribution) reflects the fact that Boltzmann's equation is *time irreversible*, in contrast with the particle system: we refer to Paragraph 1.3 below for more on this point.

## 1.2. Existence theories

In this paragraph we give a short presentation of three approaches to solving the Cauchy problem (1): the question is to know whether given  $f^0$ , there exists a unique solution to the equation, and what is its life span.

*Renormalised solutions.* — For many partial differential evolution equations, a natural approach to constructing solutions is to exploit the a priori controls provided by the equation in order to design an approximation scheme.

We have presented in the previous paragraph the conservation laws associated with the Boltzmann equation (1). Unfortunately such a priori information on the solution, typically the log-linear bound (5) — also known as an  $L \log L$  bound — is not sufficient to make sense of the collision term which is quadratic. By introducing a notion of *renormalised solution* (a function with bounded entropy satisfying a formally equivalent equation obtained by taming concentrations) and exploiting the entropy inequality (5), DiPerna and Lions (1989) nevertheless succeeded in proving the *global existence* of renormalised solutions to (1). However, their uniqueness is not known to date, nor the fact that they satisfy (1) even in the sense of distributions.

*Fixed-point methods.* — In such a situation where the a priori bound does not provide enough information to conclude, the strategy usually employed is to change perspective and consider the PDE as a fixed point problem to be solved. More precisely, using the so-called Duhamel formula we can rewrite the equation (1) in integrated form:

$$(6) \quad \begin{aligned} f(t) &= \mathcal{S}_t f^0 + \mathcal{B}_t(f(t), f(t)), \\ \mathcal{B}_t(f(t), f(t)) &\coloneqq \int_0^t \mathcal{S}_{t-s} Q(f(s), f(s)) ds, \end{aligned}$$

where  $\mathcal{S}_t$  is the free transport operator that attaches to any function  $g$  on  $\mathbb{R}^{2d}$  the function

$$\mathcal{S}_t g(x, v) \coloneqq g(x - vt, v).$$

Solving (6) reduces to looking for a Banach space in which the operators  $\mathcal{S}_t$  and  $\mathcal{B}_t$  operate continuously. A typical result, based on the Cauchy-Kowalewskaya theorem (as in Treves (1970) or Nirenberg (1972) for instance) states that if  $f^0$  is a continuous function in a weighted space  $L_\beta^\infty$  in velocities, meaning that  $f^0$  is continuous on  $\mathbb{R}^{2d}$  and satisfies

$$(7) \quad \|f_0\|_{L_\beta^\infty} \coloneqq \left\| f_0 \exp\left(\frac{\beta}{2}|v|^2\right) \right\|_{L^\infty(\mathbb{R}^{2d})} < \infty$$

for some  $\beta > 0$ , then there exists a constant  $C_\beta > 0$  (depending only on  $\beta$ ) such that the solution of (6) has a unique continuous solution on  $[0, T]$ , with

$$T = \frac{C_\beta}{\left\| f_0 \exp\left(\frac{\beta}{2}|v|^2\right) \right\|_{L^\infty(\mathbb{R}^{2d})}}.$$

Actually not only is the solution continuous, but it is also stable with respect to perturbations of the initial data, in the same function space. Unlike the renormalised solutions framework presented above, this type of result does not make any use of the particular structure of the nonlinear term (especially of the cancellations between the gain and loss terms): it suffices for the nonlinear term to be quadratic and to produce a linear loss in velocity (actually this loss is triggered by the defect of integrability in (4) for large relative velocities  $v - v_*$ ).

To exaggerate somewhat, by this method one is roughly solving an equation of the type

$$\partial_t f = f^2.$$

Such an equation is of course known to have a solution blowing up in finite time, so the only way to improve the well-posedness of (6) is to use more information on the structure of the nonlinear term.

*Perturbative methods.* — Using the entropy seems difficult as it provides too little a priori smoothness and decay on the solution, so a third strategy consists in exploiting known global solutions and then to act perturbatively. For instance, since the Maxwellian

$$M_\beta(v) := \frac{\beta^{d/2}}{(2\pi)^{\frac{d}{2}}} \exp\left(-\beta \frac{|v|^2}{2}\right)$$

is a stationary solution, one can try to solve (6) in the vicinity of  $M_\beta$ . Assuming the initial data takes the form

$$f^0 = M_\beta(1 + g^0)$$

with  $g^0$  smooth and small enough in an appropriate function space (with strong enough decay in velocities), then one can produce a unique solution  $f(t) = M_\beta(1 + g(t))$  for all positive times (Ukai, 1974). This approach crucially uses the fact that the collision operator  $2Q(M_\beta, \cdot)$  is coercive in  $L^2(M_\beta^{-1} dv)$ , which is inherited from the dissipative nature of the equation. Another possibility is considering solutions which do not depend on the space variable (Carleman, 1932).

### 1.3. The Loschmidt paradox and the loss of information

What went down in history as the most famous criticism of Boltzmann's theory is an argument due to Loschmidt (1876) (see Cercignani, 1998, for an historical account). It confronts two indisputable facts: the microscopic laws of classical mechanics are reversible, yet the kinetic world displays an arrow of time, as the H-Theorem indeed shows.

The apparent contrast can be interpreted as related to information: the irreversible evolution corresponds to a gradual loss of microscopic detail. Entropy measures the level of information, and the entropy production quantifies the amount of information discarded when the complete microscopic state of the particle system is replaced by a reduced statistical description.

In fact, a mathematical investigation of the transition from particle systems to the kinetic description allows one to complement this discussion with a more pragmatic perspective. It allows indeed to quantify the defect of chaos (see Section 3.2 below), and to relate the entropy production to the growth of microscopic correlations (see Spohn, 1997).

## 2. Short time derivation

In this section we shall present Lanford's theorem, which ensures the validity of the Boltzmann equation (1) starting with a system of hard spheres, for a short time. It also provides a control on correlations, and therefore on the chaos approximation, i.e. the asymptotic factorisation of the correlation functions.

### 2.1. The hard-sphere system and the Liouville equation

We assume throughout that the gas is made of small identical particles, which are spheres of diameter  $\varepsilon \ll 1$  interacting only through contact (see Figure 2). This is referred to as a *hard-sphere gas*. If the gas consists of  $N$  particles, its state is described by

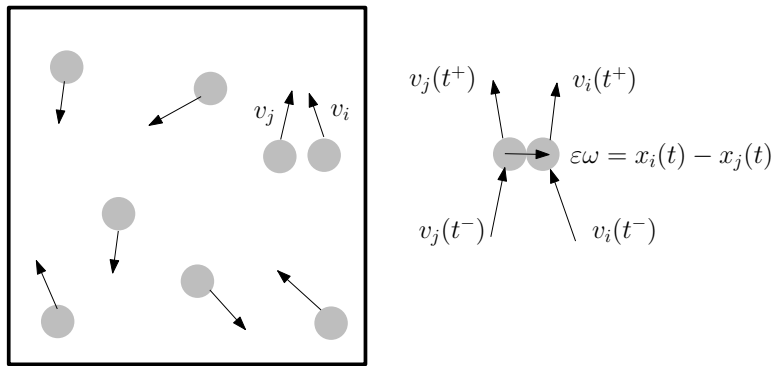


FIGURE 2. The hard-sphere dynamics and the deflection condition.

the collection  $(x_1, \dots, x_N) \in \mathbb{R}^{dN}$  of their positions and the collection  $(v_1, \dots, v_N) \in \mathbb{R}^{dN}$  of their velocities. Knowing the state of the gas at a certain instant (say  $t = 0$ ), we can describe its state at any time  $t \in \mathbb{R}$  by solving the following system of ordinary differential equations:

$$(8) \quad \frac{dx_i}{dt} = v_i, \quad \frac{dv_i}{dt} = 0 \quad \text{as long as } |x_i(t) - x_j(t)| > \varepsilon \quad \text{for } 1 \leq i \neq j \leq N,$$

with specular reflection condition at each collision: if  $|x_i(t) - x_i(t^-)| = \varepsilon$ , then

$$(9) \quad \begin{cases} v_i(t^+) := v_i(t^-) - ((v_i(t^-) - v_j(t^-)) \cdot \omega) \omega \\ v_j(t^+) := v_j(t^-) + ((v_i(t^-) - v_j(t^-)) \cdot \omega) \omega \end{cases}$$

where  $\omega := (x_i(t) - x_j(t))/\varepsilon$  is the unit vector in the direction of the relative positions at the collision time  $t$ . As pointed out in (2)-(3), this condition ensures that the collisions are elastic: momentum and energy are conserved. Note that (8) has a unique global solution  $((x_1, \dots, x_N)(t), (v_1, \dots, v_N)(t))$  outside a set of initial data which has Lebesgue measure zero (see Alexander, 1976, for example).

The dynamics of the particles is deterministic, and we choose the initial state of the gas randomly following a grand-canonical formalism (see, for example, Ruelle, 1969). The grand-canonical formalism is known to be technically convenient when dealing with correlations at low density (see van Beijeren, Lanford, Lebowitz, and Spohn, 1980).

We therefore assume that the number of particles  $\mathcal{N}$  in the gas is random, with a Poisson-like distribution with parameter  $\mu_\varepsilon > 0$  to be determined. Given  $N$  particles, we denote by  $\mathbf{x}_N := (x_1, \dots, x_N)$  in  $\mathbb{R}^{dN}$  the vector representing the position of each of these particles and by  $\mathbf{v}_N := (v_1, \dots, v_N)$  in  $\mathbb{R}^{dN}$  the vector representing their velocities. We set  $\mathbf{z}_N := (\mathbf{x}_N, \mathbf{v}_N)$ . As a shorthand notation we shall write also  $\mathbf{z}_H$  for the set  $(z_i)_{i \in H}$  when  $H$  is a subset of  $\{1, \dots, N\}$ . For simplicity let us assume that the initial density distribution  $W_N^{\varepsilon,0}$  corresponds to almost independent and identically distributed particles

$$(10) \quad \frac{1}{N!} W_N^{\varepsilon,0}(\mathbf{z}_N) := \frac{1}{\mathcal{Z}^\varepsilon} \frac{\mu_\varepsilon^N}{N!} \mathbf{1}_{\mathcal{D}_N^\varepsilon}(\mathbf{z}_N) \prod_{i=1}^N f^0(z_i),$$

where  $\mathcal{D}_N^\varepsilon$  encodes the exclusion condition

$$\mathcal{D}_N^\varepsilon := \left\{ \mathbf{z}_N \in \mathbb{R}^{2dN} : |x_i - x_j| > \varepsilon \ \forall i \neq j \right\}$$

and the partition function is defined by

$$(11) \quad \mathcal{Z}^\varepsilon := 1 + \sum_{N \geq 1} \frac{\mu_\varepsilon^N}{N!} \int_{\mathcal{D}_N^\varepsilon} d\mathbf{z}_N \prod_{i=1}^N f^0(z_i).$$

Note that the small correlation due to the initial exclusion is harmless in the analysis that will follow and we will ignore it most of the time. The distribution of a single particle  $f^0$  is assumed to be a continuous and Lipschitz probability density on  $\mathbb{R}^{2d}$  satisfying (7) for some  $\beta > 0$ .

The probability of an event  $A$  relative to the measure (10) will be denoted by  $\mathbb{P}_\varepsilon(A)$ , and  $\mathbb{E}_\varepsilon$  will be the expectation. In particular, the expectation of the number of particles  $\mathcal{N}$  is determined asymptotically by  $\mu_\varepsilon$  in the sense that

$$\lim_{\varepsilon \rightarrow 0} \mu_\varepsilon^{-1} \mathbb{E}_\varepsilon[\mathcal{N}] = 1.$$

We assume from now on that the gas is *dilute* by setting

$$(12) \quad \mu_\varepsilon = \varepsilon^{-(d-1)}.$$

Since the size of a cylinder based on a sphere of diameter  $\varepsilon$  is proportional to  $\varepsilon^{d-1}$ , this choice of scaling guarantees that the mean free time between collisions of a given particle is of the order of one, meaning that it is essentially independent of  $\varepsilon$ .

The Newtonian system satisfied by the particles translates, at the level of the distribution function  $W_N^\varepsilon(t)$  for all times  $t$ , into the following Liouville equation

$$(13) \quad \partial_t W_N^\varepsilon + \mathbf{v}_N \cdot \nabla_{\mathbf{x}_N} W_N^\varepsilon = 0 \quad \text{in } \mathcal{D}_N^\varepsilon,$$

with specular reflection condition at the boundary of  $\mathcal{D}_N^\varepsilon$ .

## 2.2. Lanford's theorem

We are interested in the typical behaviour of a particle in the hard-sphere gas. We recall that, according to the grand-canonical description given in Section 2.1, the randomness comes through the initial configuration of particles  $(z_1(0), \dots, z_N(0))$ , chosen according to the probability measure (10). The main object of investigation becomes then the discrete random field

$$(14) \quad \Pi^\varepsilon(h, t) := \frac{1}{\mu_\varepsilon} \sum_{i=1}^N h(z_i(t))$$

defined on bounded test functions  $h \in C^0(\mathbb{R}^{2d})$ . This random field is introduced, by following the original intuition of Boltzmann, to “count” the number of particles in little boxes of the one-particle phase space  $\mathbb{R}^{2d}$ . The scope of Lanford's theorem is to prove a law of large numbers for this random field; namely that its distribution concentrates, as  $\varepsilon \rightarrow 0$ , to the deterministic limit driven by the Boltzmann equation:

$$(15) \quad \Pi^\varepsilon(h, t) \rightarrow \int_{\mathbb{R}^{2d}} f(t) h(x, v) dx dv.$$

To do this, we are led to study the first and second moments of  $\Pi^\varepsilon$ , that means in particular computing the expectation (with respect to (10))

$$(16) \quad \mathbb{E}_\varepsilon [\Pi^\varepsilon(h, t)] =: \int_{\mathbb{R}^{2d}} f_1^\varepsilon(t, x, v) h(x, v) dx dv$$

where the right hand side defines the first correlation function  $f_1^\varepsilon$ . Due to the invariance under permutations of the density distribution  $W_N^\varepsilon(t)$ , it is not hard to see that this amounts to studying its projection on the one-particle space:

$$(17) \quad f_1^\varepsilon(t, z_1) = \frac{1}{\mu_\varepsilon} \sum_{p=0}^{\infty} \frac{1}{p!} \int dz_2 \dots dz_{p+1} W_{p+1}^\varepsilon(t, \mathbf{z}_{p+1}).$$

The evolution of  $f_1^\varepsilon(t)$  over time is therefore dictated by that of  $W_N^\varepsilon(t)$  for all integers  $N$ . It is also easy to see that the equation satisfied by  $f_1^\varepsilon$  is not closed : if we define the correlation function of order  $k$  to be the joint probability of  $k$  typical, selected particles

$$(18) \quad \begin{aligned} & \mathbb{E}_\varepsilon \left[ \frac{1}{\mu_\varepsilon^k} \sum_{(i_1, i_2, \dots, i_k)} h(z_{i_1}(t), z_{i_2}(t), \dots, z_{i_k}(t)) \right] \\ & =: \int_{\mathbb{R}^{2dk}} f_k^\varepsilon(t, z_1, \dots, z_k) h(z_1, \dots, z_k) dz_1 \dots dz_k \end{aligned}$$

then the equation satisfied by  $f_1^\varepsilon$  involves the second correlation function  $f_2^\varepsilon$ , whose equation itself involves  $f_3^\varepsilon$ , and so on. We more generally obtain that the equation on  $f_k^\varepsilon$  can be written

$$(19) \quad \partial_t f_k^\varepsilon + \mathbf{v}_k \cdot \nabla_{\mathbf{x}_k} f_k^\varepsilon = C_{k,k+1}^\varepsilon f_{k+1}^\varepsilon \quad \text{in } \mathcal{D}_k^\varepsilon,$$

with a specular reflection condition at the boundary of  $\mathcal{D}_k^\varepsilon$ . This set of equations on  $(f_k^\varepsilon)_{k \geq 1}$  is referred to as the BBGKY hierarchy. The collision operator  $C_{k,k+1}^\varepsilon$  comes from the boundary term in Green's formula and is defined as follows:

$$(20) \quad \begin{aligned} (C_{k,k+1}^\varepsilon f_{k+1}^\varepsilon)(\mathbf{z}_k) &:= \sum_{i=1}^k \int f_{k+1}^\varepsilon(\mathbf{z}_k^{\langle i \rangle}, x_i, v'_i, x_i + \varepsilon\omega, w') \left( (w - v_i) \cdot \omega \right)_+ d\omega dw \\ &\quad - \int f_{k+1}^\varepsilon(\mathbf{z}_k^{\langle i \rangle}, x_i, v_i, x_i + \varepsilon\omega, w) \left( (w - v_i) \cdot \omega \right)_- d\omega dw, \end{aligned}$$

where  $(v'_i, w')$  is recovered from  $(v_i, w)$  through the scattering laws (9), and with the notation

$$\mathbf{z}_k^{\langle i \rangle} := (z_1, \dots, z_{i-1}, z_{i+1}, \dots, z_k).$$

Note that if  $C_{1,2}$  denotes the formal limit of  $C_{1,2}^\varepsilon$  as  $\varepsilon$  goes to zero, then the right-hand side  $Q(f, f)$  of the Boltzmann equation (4) is none other than  $C_{1,2}(f^{\otimes 2})$ .

The key result derived by Lanford (1975) is the convergence for short times of  $f_1^\varepsilon(t)$  to  $f(t)$ , the solution of the Boltzmann equation with initial data  $f^0$ .

**THEOREM 2.1** (Lanford, 1975). — *Under assumption (7), there exists a time  $T_L > 0$  depending on  $C_0$  and  $\beta$  such that, for any  $t \in [0, T_L]$ ,*

$$(21) \quad \lim_{\varepsilon \rightarrow 0} f_1^\varepsilon(t) = f(t)$$

*uniformly in  $\mathbb{R}^{2d}$ .*

*Remark 2.2* (More on Lanford's convergence result). — The formula (10) for the initial data is a specific choice, which is adopted here merely for the sake of simplicity. Lanford (1975, 1976) discussed the initial conditions much more thoroughly. He gave conditions characterising a typical initial state for which Theorem 2.1 holds.

The convergence (21) actually holds in a weighted space similar to (7) but with a deteriorated parameter  $\beta$  (indeed  $f_1^\varepsilon(t)$  is shown to decay as  $M_{\beta(t)}$  with  $\beta(t)$  decaying linearly in time).

*Remark 2.3* (On the propagation of chaos). — Since the evolution of  $f_1^\varepsilon$  involves the whole BBGKY hierarchy, the proof actually shows that  $f_k^\varepsilon(t)$  converges to  $f^{\otimes k}(t)$  on the same time interval, almost everywhere in  $\mathbb{R}^{2dk}$ : the initial chaos property  $f_k^\varepsilon(0) \sim (f^0)^{\otimes k}$  satisfied by (10) is therefore asymptotically preserved on  $[0, T_L]$ . Using that, for  $k \geq 2$ , the correlation functions are linked to the higher order moments of the field  $\Pi^\varepsilon$ , this implies also the stronger statement (15), i.e. the convergence in probability of the empirical measure (see Spohn, 1991).

Nowadays, we are able to control much more detailed information about the random field  $\Pi^\varepsilon$ , such as its local Poissonian statistics, small fluctuations (including a central limit theorem), and large deviations from the typical behavior; see Section 5 for related considerations.

*Remark 2.4* (On the time restriction). — The main drawback of the result is the time restriction  $T_L$ : it can be checked that this time is of the same order as the time  $T$  on which a fixed point method allows to solve the Boltzmann equation (see Section 1.2). The achievement of the main result presented in this paper (Theorem 4.1 below) is that  $T_L$  can be replaced by the time on which the Boltzmann equation has a smooth solution, regardless of the way such a solution is constructed. See Section 4 for more on this.

### 2.3. A strategy of the proof

Lanford's proof, progressively refined and made more quantitative by many authors over the years, is nowadays a classical argument in perturbation theory: we refer for instance to Uchiyama (1988), Spohn (1991), Cercignani, Illner, and Pulvirenti (1994), Cercignani, Gerasimenko, and Petrina (1997), Ukai (2001), Gallagher, Saint-Raymond, and Texier (2014), and Pulvirenti, Saffirio, and Simonella (2014). The original proof is built upon the hard-sphere hierarchy (19). The guiding idea is:

(0') Express the correlation function  $f_1^\varepsilon(t)$  in terms of the initial correlation functions  $f_k^\varepsilon(0)$ , using a series expansion in “collision histories”, labelled by binary tree graphs, obtained by iterating the Duhamel formula associated with (19) backwards in time. Each term corresponds to the backward flow of a finite group of particles that are successively added in a collisional configuration and then evolve under the reduced hard-sphere dynamics.

The argument then proceeds in three steps.

- (1') Prove that, for sufficiently short times, the series expansion of  $f_1^\varepsilon(t)$  constructed in Step (0') is absolutely convergent, uniformly in  $\varepsilon$ , in weighted  $L^\infty$  spaces such as (7).
- (2') Prove that in the low-density scaling (12), almost all collision histories have no recollision, meaning that no collision occurs other than the ones prescribed by the collision tree constructed in Step (0').

(3') The rest of the argument is simple: neglecting recollisions, the measure of which tends to zero, one sees that the expansion reduces termwise to the iterated Duhamel formula for the Boltzmann equation, and by inspection that  $f_k^\varepsilon(t) \rightarrow f^{\otimes k}(t)$  when  $\varepsilon \rightarrow 0$ .

The proof we present in Section 3 below is not the original proof by Lanford, though the two proofs share many similarities. The main difference lies in the way the functions  $f_k^\varepsilon(t)$  are explicitly represented. In place of a backward iterated formula, the guiding idea is a *cluster expansion* of trajectories as in (Bodineau, Gallagher, Saint-Raymond, and Simonella, 2022), in turn inspired from previous work on cumulant methods (Pulvirenti and Simonella, 2017; Bodineau, Gallagher, Saint-Raymond, and Simonella, 2023b). The plan is the following:

- (0) Implement a *dynamical cluster expansion* associated to the hard-sphere dynamics. This leads to express  $f_k^\varepsilon(t)$  as an expansion over cluster trajectories labelled by complex *collision graphs* (encoding all possible interactions between the particles).
- (1) Obtain uniform bounds on the expansion (as in (1') above).
- (2) Reduce to minimally connected (tree) graphs, by showing that one can discard recollisions. This implies the chaos property as in (2') above.
- (3) Identify the Boltzmann equation after the limit  $\varepsilon \rightarrow 0$ .

Overall, the cluster expansion strategy is more complicated than Lanford's original method. In fact, it requires to understand and exploit subtle cancellations among graphs with different signs (both in Steps (1) and (3)). The interest of presenting this strategy is that it prepares for the proof of the main result of this paper in Section 4, which will overcome the time restriction to  $[0, T_L]$  arising from Step (1).

### 3. Proof of Lanford's theorem using cluster expansions

#### 3.1. A pictorial proof of Steps (0) to (3)

In this paragraph, we provide pictorial explanations of the main steps of the proof of Theorem 2.1. For more details, we refer to Bodineau, Gallagher, Saint-Raymond, and Simonella (2022).

**Step (0).** — Starting from an initial particle configuration  $\mathbf{z}_N(0) = \mathbf{z}_N$  in  $\mathbb{R}^{2dN}$ , the collisions in the dynamics induce correlations between the particles. Given a time interval  $[0, \tau]$ , the particle evolution leads to a partition into (connected) *collision graphs*  $\lambda_1, \dots, \lambda_n$  with edges labelled by the particle indices in  $\{1, \dots, N\}$ . This is obtained by adding a vertex at the intersection of two particle paths (represented by edges) when they collide in  $[0, \tau]$  and the  $\lambda_i$  represent all the connected components obtained after this construction; see Figure 3. This representation depends strongly on the time window  $[0, \tau]$  and on the initial data. In particular the number  $n$  of collision graphs ranges from 1 to  $N$  (no collision has occurred on the time interval  $[0, \tau]$ ).

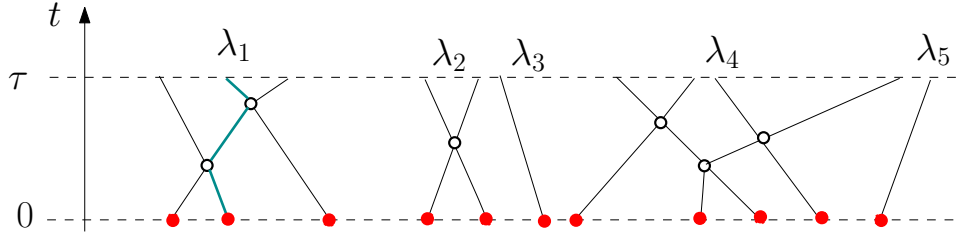


FIGURE 3. This figure encodes the hard-sphere dynamics of 11 particle trajectories during the time interval  $[0, \tau]$ . The particles (which are “independent”) at initial time are represented by red bullets and their paths by lines. A collision between 2 particles is represented by a circle and leads to a scattering of the particles : as an example, a particle trajectory is represented by the green broken line. This evolution leads to the collision graphs  $\{\lambda_1, \dots, \lambda_5\}$  which contain different numbers of particles (in particular  $\lambda_3$  and  $\lambda_5$  contain only one particle).

Notice that, in general, collision graphs are not minimally connected and may include *cycles*, as displayed in Figure 4. In this case, some of the collisions may be called “recollisions” to indicate their role in the generation of the cycles.

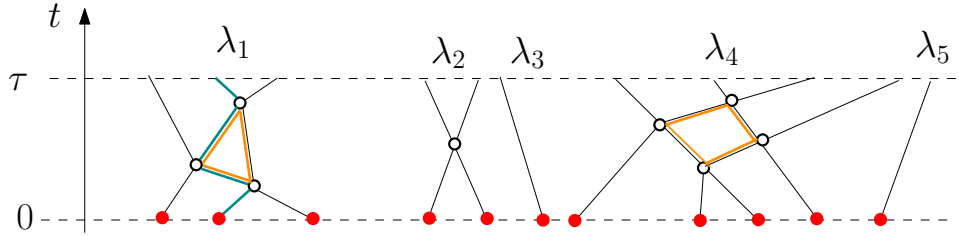


FIGURE 4. Compared to Figure 3, the collision graphs  $\lambda_1$  and  $\lambda_4$  display cycles. The top (bottom) collisions in those graphs are recollisions if we follow the cluster trajectory forward (backward) in time.

Consider now the evolution of a particle which belongs to a collision graph  $\lambda_i$ . Its trajectory can be complicated due to the collisions, however it is determined only by the particles in  $\lambda_i$  (see Figure 4). The notation  $\lambda_i$  will refer not only to a collision graph, but also to the coordinates of the particles indexed by the edges of  $\lambda_i$  and their time evolution. In this way, there is a one-to-one correspondence between an initial configuration  $\{\mathbf{z}_N\}$  and a decomposition  $\{\lambda_1, \dots, \lambda_n\}$ . This will allow us to change our point of view and, instead of the grand-canonical measure  $W_N^\varepsilon$  with initial datum given in (10), to study a measure on collision graphs

$$(22) \quad \frac{1}{n!} \widetilde{W}_n^\varepsilon(\lambda_1, \dots, \lambda_n) := \frac{1}{\mathcal{Z}^\varepsilon} \frac{1}{n!} \prod_{i=1}^n \nu^\varepsilon(\lambda_i) \prod_{i \neq j} \mathbf{1}_{\lambda_i \neq \lambda_j}, \quad n \geq 0,$$

where

$$(23) \quad \nu^\varepsilon(\lambda) := \frac{\mu_\varepsilon^{|\lambda|}}{|\lambda|!} (f^0)^{\otimes |\lambda|} \mathbf{1}_{\lambda \text{ is a collision graph}} d\mathbf{z}_{|\lambda|}.$$

We will not define formally this measure, but intuitively  $\tilde{W}_n^\varepsilon$  has a structure similar to  $W_N^\varepsilon$ : instead of choosing particles with density  $f^0$ , each collision graph is chosen according to a density  $\nu^\varepsilon$  which will determine the number of particles in the graph as well as the corresponding coordinates so that their trajectories satisfy the collision constraints imposed by the graph. By definition, the dynamics should depend only on the particles within each graph, thus the measure (22) has also an exclusion condition as the trajectories in different collision graphs  $\lambda_i, \lambda_j$  should not approach at a distance less than  $\varepsilon$ . This is denoted by  $\lambda_i \not\sim \lambda_j$  and is the counterpart of the exclusion term  $\mathbf{1}_{\mathcal{D}_N^\varepsilon}$  in (10). Finally  $|\lambda|$  denotes the number of particles in  $\lambda$ , which we shall refer to as the *size* of  $\lambda$ .

In the Boltzmann–Grad scaling (12), a typical particle undergoes one collision per unit time, thus in a small time interval  $[0, \tau]$ , with  $\tau$  smaller than the mean free time between collisions:

- the size of a collision graph is expected to be of order 1, and therefore the corresponding trajectories should remain simple<sup>(4)</sup>. A few collision graphs will be as large as  $\log \mu_\varepsilon$ , but on the whole, their distribution is well behaved;
- the exclusion condition is a weak constraint and will hold outside a negligible set, meaning that the initial configurations leading to a violation of this condition will have vanishing probability as  $\varepsilon$  goes to zero.

The *cluster expansion* method is a well established perturbation theory devised originally to study the equilibrium Gibbs distributions of weakly interacting gases. This versatile tool has then been applied in a variety of cases (see e.g. Poghosyan and Ueltschi, 2009) and we will implement it here to study the weakly interacting collision graphs (which already encode the dynamical information)<sup>(5)</sup>.

The interaction in the measure (22) comes from the dynamical exclusion condition which we are going to rewrite as

$$(24) \quad \prod_{\substack{i,j \leq n \\ i \neq j}} \mathbf{1}_{\lambda_i \not\sim \lambda_j} = \prod_{\substack{i,j \leq n \\ i \neq j}} (1 - \mathbf{1}_{\lambda_i \sim \lambda_j}),$$

where  $\lambda_i \sim \lambda_j$  means that the collision graphs *overlap*, i.e. that two particles from each collision graph must meet in the time interval  $[0, \tau]$ , as in Figure 5. An overlap is not a collision and it does not modify the microscopic dynamics, it is just a convention to represent the complement of  $\{\lambda_i \not\sim \lambda_j\}$ : overlaps represent fictitious dynamics, where particles from different collision graphs can cross each other.

<sup>(4)</sup> Here the smallness of  $\tau$  is crucial: indeed it has been shown (by numerical and formal arguments) that, for  $\tau$  of the order of one mean free time, the size of collision graphs is expected to explode, by strong analogy with Erdős–Renyi random graphs with supercritical parameter (Patterson, Simonella, and Wagner, 2016, 2017).

<sup>(5)</sup>In the context of scaling (12), cluster expansion techniques have been studied intensively starting from Pulvirenti and Simonella (2017), and proved to be a natural and powerful strategy when one aims at quantifying correlations and studying fluctuations: see Bodineau, Gallagher, Saint-Raymond, and Simonella (2020, 2023b, 2024b), Le Bihan (2025a,b), and Simonella and Winter (2026).

By expanding the product (24), we will get terms of the form  $\mathbf{1}_{\lambda_{i_1} \sim \lambda_{i_2}} \mathbf{1}_{\lambda_{i_2} \sim \lambda_{i_3}}$  which should be interpreted as follows : the trajectories of the particles are fully determined by each collision graph  $\lambda_{i_1}, \lambda_{i_2}, \lambda_{i_3}$  and there are two additional geometric constraints as  $\lambda_{i_1}, \lambda_{i_2}$  and  $\lambda_{i_2}, \lambda_{i_3}$  must overlap (see Figure 5). After this expansion, the relevant objects are the *clusters*  $\sigma_i = \{\lambda_{i_1}, \dots, \lambda_{i_\ell}\}$  which are collections of collision graphs constrained to overlap. Of course, this operation will possibly lead to further cycles: this can be seen in  $\{\lambda_1, \lambda_2, \lambda_3\}$  in Figure 5 for instance, since new cycles have been created due to the overlaps  $\mathbf{1}_{\lambda_1 \sim \lambda_2} \mathbf{1}_{\lambda_2 \sim \lambda_3} \mathbf{1}_{\lambda_1 \sim \lambda_3}$ .

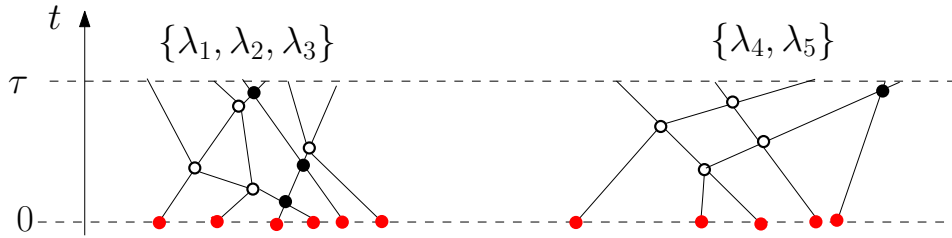


FIGURE 5. Above, the collisions graphs in Figure 4 have been associated to form two clusters : on the left  $\lambda_1, \lambda_2, \lambda_3$  are now linked by three overlaps, represented by black dots and on the right  $\lambda_4, \lambda_5$  are linked by one overlap. Note that the overlaps on the left generate one cycle.

Once the exclusion of the collision graphs has been expanded, there is no more interaction between the clusters. Thus the measure (22) can be upgraded to define a distribution on *independent* clusters. This distribution will have a structure reminiscent of a Poisson measure, however it will no longer be a probability measure as the different terms in the expansion of (24) have signs. The distribution will have the form

$$(25) \quad \frac{1}{\mathcal{Z}^\varepsilon} \frac{1}{m!} \prod_{i=1}^m \tilde{\nu}^\varepsilon(\sigma_i) \quad m \geq 0,$$

where the measure on the cluster  $\sigma = \{\lambda_1, \dots, \lambda_n\}$  is defined (using (23)) by

$$(26) \quad \tilde{\nu}^\varepsilon(\sigma) := \frac{1}{n!} \varphi_\varepsilon(\lambda_1, \dots, \lambda_n) \prod_{i=1}^n \nu^\varepsilon(\lambda_i),$$

and  $\varphi_\varepsilon$  encodes the cluster structure between the collision graphs

$$\varphi_\varepsilon(\lambda_1, \dots, \lambda_n) := \sum \prod_{\{j, j'\} \in E(G_n)} (-\mathbf{1}_{\lambda_j \sim \lambda_{j'}}),$$

where the sum runs on all connected graphs  $G_n$  with  $n$  vertices, and  $E(G_n)$  denotes the corresponding set of edges.

Now recall that the Lanford theorem is a statement on  $f_1^\varepsilon(t)$  — or more generally on the  $k$ -th correlation function  $f_k^\varepsilon(t)$ ,  $k \geq 1$ , which describes the behaviour of  $k$  typical, selected particles. One thus needs to *project* the new measure defined in (25) by computing correlation functions as in (18).

Let us detail the procedure to recover  $f_1^\varepsilon(t)$ . By (16), using the exchangeability (i.e. the symmetry of the measure under permutations), we have that

$$\int_{\mathbb{R}^{2d}} f_1^\varepsilon(t, x, v) h(x, v) dx dv \approx \mathbb{E}_\varepsilon [h(z_1(t))] .$$

The previous decomposition in clusters has two crucial properties

- The trajectory of a given particle depends only on the particles in the same cluster, in particular  $z_1(t)$  is completely prescribed by the cluster  $\sigma_1$  containing particle 1;
- The measure  $W_N^\varepsilon$  is not factorized at the level of particles, but by definition it is at the level of clusters (see (25)).

Therefore we can rewrite the previous formula as

$$\int_{\mathbb{R}^{2d}} f_1^\varepsilon(t, x, v) h(x, v) dx dv \approx \mathbb{E}_{\tilde{\nu}^\varepsilon} [h(z_1(t))] ,$$

keeping only the factor corresponding to the cluster  $\sigma_1$ , since the average of all other factors in the product (corresponding to clusters independent from particle 1) is 1. Recall that the measure  $\tilde{\nu}^\varepsilon(\sigma_1)$  is given by (23)-(26) encoding the conditioning by the geometric constraints associated to  $\sigma_1$ .

Figure 6 depicts the case of  $f_1^\varepsilon(t)$ , where the particle in green is the typical particle, the history of which we are interested in. In this case, only one connected cluster is left: all other clusters disappear from the analysis.

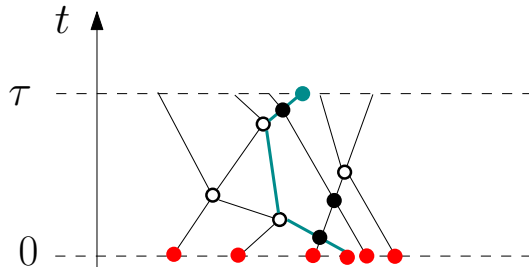


FIGURE 6. Projection leading to the distribution of a typical particle:  $f_1^\varepsilon(\tau)$  is expressed as an expansion over cluster trajectories of this form, labelled by *connected* collision graphs. The particle associated with  $f_1^\varepsilon(\tau)$  is depicted by a green circle at time  $\tau$  and its path is also green.

Of course for  $f_2^\varepsilon(t)$  (more generally  $f_k^\varepsilon(t)$ ), a similar expansion holds true, but two (or up to  $k$ ) clusters may appear in such an expansion, due to the fact that we select two (or  $k$ ) particles; see Figure 7.

From now on and in agreement with Figure 6 and the following ones, we shall call “green particles” the particles of interest, meaning those recorded in  $f_k^\varepsilon(t)$  as opposed to those appearing due to a collision/overlap.

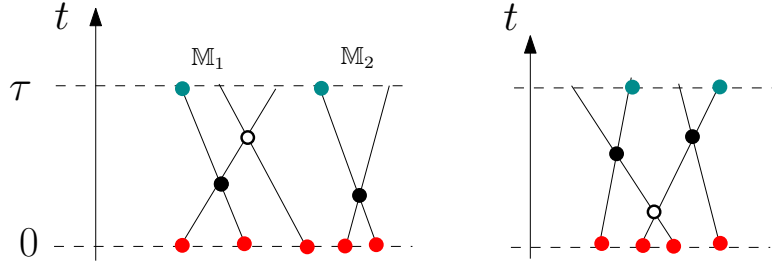


FIGURE 7. Projection leading to the distribution of two typical particles:  $f_2^\varepsilon(t)$  is an expansion over cluster trajectories that may belong either to two disconnected collision graphs (on the left), or to the same cluster (on the right).

**Step (1).** — Using the fact that the gas is dilute and the time  $\tau$  is small, one can show that typically the clusters contain only few particles, and few collisions and overlaps. Thus the corresponding distribution (22) can be studied analytically and it is well behaved.

More precisely, we want to control the norm of the functions  $f_k^\varepsilon(t)$ , or (which is a very similar task), we want to understand the behaviour of the partition function  $\overline{\mathcal{Z}}^\varepsilon$  in (25). Note that, to compute these functions, we have to sum over all possible collections of clusters and integrate over all the corresponding cluster trajectories.

First of all, one can prove an estimate on the density of collision graphs  $\nu^\varepsilon$  defined by (23) (which, recall, contain no overlaps) of the type

$$(27) \quad \sum_{\lambda} \int_{\mathbb{R}^{2d|\lambda|}} |\nu^\varepsilon(\lambda)| = O(C_0 \mu_\varepsilon),$$

provided that  $\tau \ll C_0^{-1}$  where  $C_0$  is defined by (7). This is based on geometric estimates, taking into account the negligible volume of configurations which should satisfy the  $|\lambda|-1$  independent collision constraints imposed by the graph  $\lambda$  (roughly, each such constraint is associated to a volume of order  $\mu_\varepsilon^{-1}\tau$ ).

Secondly, one has to prove an estimate on the density of clusters  $\tilde{\nu}^\varepsilon$  defined by (26). At this point, we observe that the function  $\varphi_\varepsilon$  involves all possible connected graphs on  $n$  vertices. This grows badly with  $n$ : however, these graphs appear with alternating signs in the expansion of  $\varphi^\varepsilon$  (each overlap carries a  $-1$ ). A powerful argument due to Penrose (1967) allows to cancel all the graphs with cycles, showing that the original expansion can be bounded from above by a simpler expansion running only over minimally connected graphs ( $\ell^{\ell-2}$  graphs involving  $\ell$  graphs  $\{\lambda_{i_1}, \dots, \lambda_{i_\ell}\}$ ). Using this and the geometric estimates, one arrives at a uniform bound of the type

$$(28) \quad \sum_{\sigma} \int |\tilde{\nu}^\varepsilon(\sigma)| = O(C_0 \mu_\varepsilon)$$

provided that  $\tau \ll C_0^{-1}$ . This eventually leads to

$$(29) \quad f_k^\varepsilon(\tau) \leq C^k.$$

Recalling that each  $f_k^\varepsilon(\tau)$  has been written as a sum over all possible collections of clusters, this uniform bound allows one to reduce the proof of Theorem 2.1 to the computation of the limit, graph by graph.

**Step (2).** — Here we want to prove the asymptotic propagation of chaos, i.e. that the initial independence of particles (up to exclusion) is preserved, up to an error vanishing with  $\varepsilon$ , at time  $\tau > 0$  recalling that this time is much smaller than the typical time between two collisions. This means that going forward in time from time 0 to  $\tau$ , when two particles in the cluster of a green particle meet, they must be independent at the instant before: their histories before that encounter should involve different particles altogether.

This is obviously not the case in Figure 8, since the top collision involves particles that already encountered before.

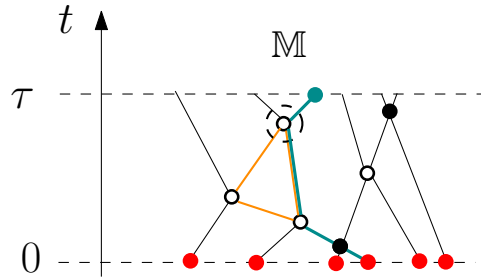


FIGURE 8. A recollision (surrounded by a dashed circle) imposes constraints on the orange part of the trajectory to form a cycle.

But actually such events are highly improbable. We have already mentioned that at time 0, each particle in the cluster is constrained to a negligible volume of order  $\mu_\varepsilon^{-1}\tau$ . Having two particles meet, although they have already interacted in the past, imposes an even stronger constraint on the velocities and deflection angles at their previous interaction, which leads to an extra decay in  $\varepsilon$ . One can prove that in the set of all cluster trajectories of the green particle, the main order term corresponds to clusters with no cycles at all, meaning trees as in Figure 9.

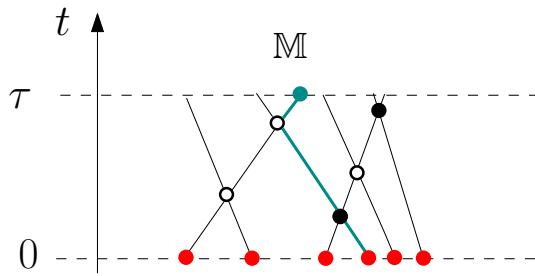


FIGURE 9. Graph (molecule) of leading type in the computation of  $f_1^\varepsilon(t)$ .

A very similar argument shows that, in the limit of  $f_2^\varepsilon(t)$  (see Figure 7 left case), not only are cycles absent, but the two green particles cannot, asymptotically, belong to a

single connected graph. In other words, the leading contributions come only from clusters with two disconnected components ( $\mathbb{M}_1, \mathbb{M}_2$ ), the first containing the green particle 1 and the second containing the green particle 2. As the components  $\mathbb{M}_1$  and  $\mathbb{M}_2$  are independent from each other, this leads to the factorisation  $f_2^\varepsilon(t) \rightarrow f(t) \otimes f(t)$  for  $\varepsilon \rightarrow 0$  (see Step (3) below).

*Remark 3.1.* — The technique developed in (Deng, Hani, and Ma, 2024) represents a highly detailed quantitative version of the estimates for clusters with cycles, where it will be shown that, as the number of cycles increases, the corresponding clusters contribute progressively less.

Consider for instance Figure 8, corresponding to a cluster which we denote  $\mathbb{M}$ . In the work by Deng, Hani and Ma, clusters of such type are called *molecules*. They are represented by graphs with edges given by the particles and with vertices associated with collisions or overlaps, with possible cycles generated by collisions (vertices of type  $\circ$ ). The orange cycle is the basic example of a  $\{33\}$  *molecule* which will be the elementary pattern to gain smallness (we refer to Section 4.4 for more).

**Step (3).** — To conclude, we need to prove that  $f_1^\varepsilon(t)$  is close to the solution of the Boltzmann equation (1), i.e to identify its limit  $f$  as the solution to (1). This means in essence relating Figure 9 to the nonlinear PDE (1). As mentioned previously, a natural expansion of the solution of (1) over trajectories is obtained by simply iterating the Duhamel formula. Due to the quadratic character of the collision operator, this leads to binary tree graphs.

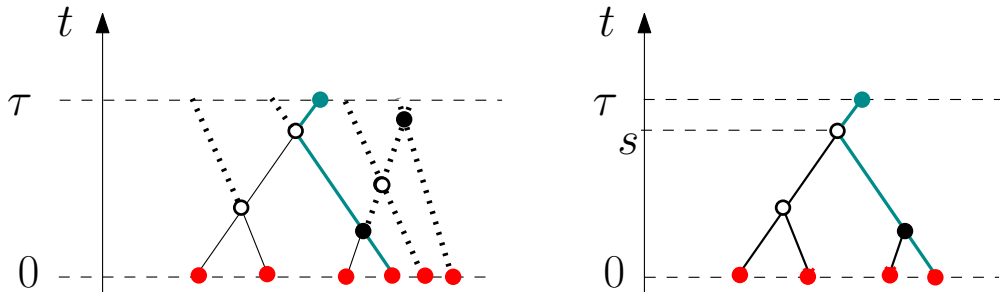


FIGURE 10. On the left, the trajectory of a tagged particle is depicted in green and the part of the cluster which is not involved in this trajectory is represented in dashed lines. At the analytical level, the contributions of the dashed lines cancel and the only relevant part of the cluster is the tree represented in the right picture. In the backward direction the tagged trajectory is modified by a collision (at time  $s$ ) determined by two independent trees in  $[0, s]$ . This is the factorisation property from which Boltzmann equation can be recovered.

The key point here is to prove that from any tree graph left by Step (2) above (see Figure 9), one can extract a binary tree by following the history of the green particle backward in time, and keeping only the particles that collided directly or indirectly

with the green particle, moving backwards. This leads to Figure 10 where the forgotten pieces of trajectory are represented by dashed lines.

Is the omission of the dashed part allowed? The answer is affirmative and can be proved by cancellations between graphs with different signs. For instance, in Figure 10 the dashed paths encounter in an overlap  $\bullet$ , which carries a minus sign. This cancels exactly with the same graph where the  $\bullet$  is replaced by a  $\circ$  corresponding to a collision.

### 3.2. Quantification of the chaos property

The chaos property can be made more quantitative by studying more precisely the convergence of  $f_k^\varepsilon(t)$  to a tensorised structure. For instance arguing as above, it is not difficult to prove that

$$(30) \quad f_2^\varepsilon(t) - f_1^\varepsilon \otimes f_1^\varepsilon(t) = O(\mu_\varepsilon^{-1})$$

for short times, in  $L^1$  norm (see the right part of Figure 7). A similar estimate is valid for  $f_k^\varepsilon - (f_1^\varepsilon)^{\otimes k}$  at least for finite (or slowly diverging) values of  $k$ .

We would like to introduce now *correlation errors* which isolate and quantify the departure from chaos, by means of new functions  $E_k^\varepsilon(t)$  with the property that  $E_k^\varepsilon(t)$  vanishes if and only if the  $k$  particles are all independent. The decay of  $E_k^\varepsilon(t)$  with  $\varepsilon$  should control precisely how far the microscopic dynamics remains from the tensorised Boltzmann one, providing a bridge between the existence of the solution  $f(t)$  and the validity of the kinetic limit. This method was introduced in (Pulvirenti and Simonella, 2017) and inspired from previous works on stochastic particle systems by De Masi and Presutti (1991) and Caprino, De Masi, Presutti, and Pulvirenti (1991)<sup>(6)</sup>.

To understand the correlations intuitively, recall that the  $k$ -point correlation function  $f_k^\varepsilon(t, z_1, \dots, z_k)$  is determined by projecting on the clusters containing the particles indexed by  $K = \{1, \dots, k\}$  at time  $t$ . At leading order each tagged particle is associated with a different cluster and  $f_k^\varepsilon$  factorises in the low-density limit. Correlations emerge between two particles when they belong to the same cluster, see Figure 11. The projection on the clusters splits the particles indexed by  $K$  into two sets: particles in  $H \subset K$  belong to a cluster containing at least another particle in  $H$ , whereas each particle in  $K \setminus H$  is associated with a cluster without any other tagged particle. The correlation can then be decomposed as

$$(31) \quad f_k^\varepsilon(t, \mathbf{z}_K) = \sum_{H \subset K} (f_1^\varepsilon)^{\otimes K \setminus H}(t) E_H^\varepsilon(t),$$

where  $\{E_h^\varepsilon\}_{h \geq 2}$  are the *correlation errors*. Here we use the abbreviated notation  $(f_1^\varepsilon)^{\otimes K \setminus H}(t) = (f_1^\varepsilon)^{\otimes (k-|H|)}(t, \mathbf{z}_{K \setminus H})$ , and  $E_H^\varepsilon(t) = E_{|H|}^\varepsilon(t, \mathbf{z}_H)$ . The functions  $f_1^\varepsilon$

<sup>(6)</sup>In (Caprino, De Masi, Presutti, and Pulvirenti, 1991), a similar method (therein called the method of *v-functions*), proved effective to overcome Lanford's short time restriction, for a kinetic limit on a lattice.

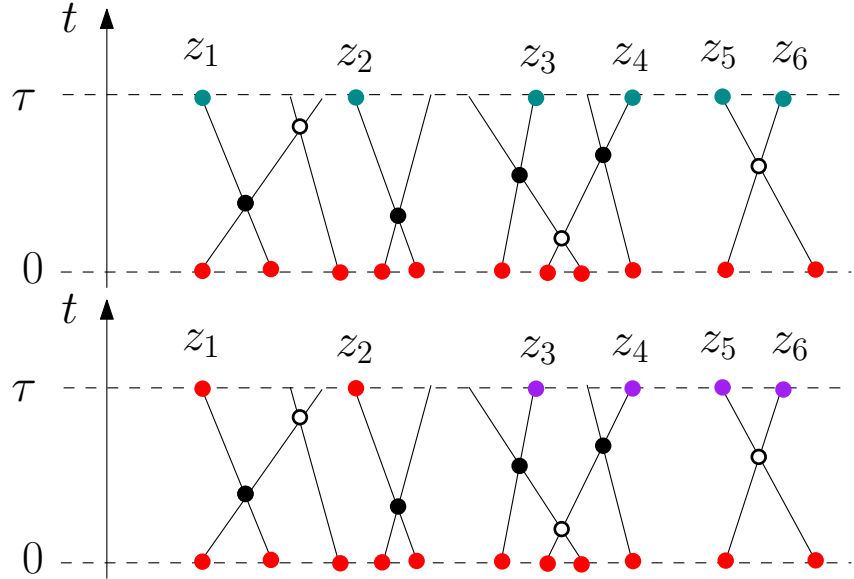


FIGURE 11. In the top figure, representing a contribution to  $f_6^\varepsilon$ , particles 1, 2 belong to two independent clusters, instead the trajectories of particles 3, 4 (respectively 5, 6) are correlated by the constraint of belonging to the same cluster. Such a configuration cluster will contribute to a term of the type  $f_1^\varepsilon(t, z_1) f_1^\varepsilon(t, z_2) E_H^\varepsilon(t, z_3, z_4, z_5, z_6)$  in (31) with  $H = \{3, 4, 5, 6\}$ . To indicate this contribution, we update the colours in the bottom figure: red bullets indicate particles which are uncorrelated (their distribution will approximate the solution of the Boltzmann equation), while purple bullets indicate particles associated to the correlation error. Ultimately the distribution at time  $\tau$  is obtained by integrating over the initial variables which are depicted by red bullets and are distributed according to a product measure  $f^0$  (as the initial correlations can be ignored by assumption).

and  $E_H^\varepsilon$  are obtained by summing over all the clusters compatible with the corresponding dynamical constraints. Note that the correlation error  $E_j^\varepsilon$  can be also defined directly from  $(f_\ell^\varepsilon)_{\ell \leq j}$  and in particular the first terms are

$$E_2^\varepsilon = f_2^\varepsilon - f_1^\varepsilon \otimes f_1^\varepsilon, \quad E_3^\varepsilon = f_3^\varepsilon - \sum f_2^\varepsilon \otimes f_1^\varepsilon + 2f_1^\varepsilon \otimes f_1^\varepsilon \otimes f_1^\varepsilon.$$

Intuitively,  $E_j^\varepsilon$  gathers all particles with some correlations, possibly distributed among several clusters: for instance, in Figure 11, particles 3, 4 and 5, 6 do not belong to the same cluster and the two pairs are independent.

The correlation errors are therefore much smaller than  $f_k^\varepsilon - (f_1^\varepsilon)^{\otimes k}$  and Pulvirenti and Simonella (2017) proved that, for suitable constants  $\alpha, \gamma \in (0, 1)$  and  $C > 0$ ,

$$(32) \quad \int |E_H^\varepsilon(t, \mathbf{z}_K)| d\mathbf{v}_H \leq C \varepsilon^{\gamma|H|}, \quad |H| < \varepsilon^{-\alpha}, \quad 0 \leq t < \tau.$$

Hence, groups of up to  $\varepsilon^{-\alpha}$  particles behave independently, up to an exponentially small error.

Once the first correlation function  $f_1^\varepsilon(\tau)$  has been approximated by the solution of the Boltzmann equation  $f(\tau)$ , one will be able to rewrite (31) up to an error (vanishing with  $\varepsilon$  in  $L^1$ ) as

$$(33) \quad f_k^\varepsilon(\tau, \mathbf{z}_K) = \sum_{H \subset K} f^{\otimes K \setminus H}(\tau) E_H^\varepsilon(\tau) + \text{error}.$$

We shall call this a *cumulant expansion* of  $f_k^\varepsilon(\tau)$ . As we shall see in Section 4, a similar cumulant expansion of the correlation functions provides a convenient ansatz to be propagated to times longer than  $\tau$ . Once the tensorised component is known to approximately satisfy the Boltzmann equation, and assuming that the solution of the Boltzmann equation is smooth, controlling the growth and decay of the  $E_j^\varepsilon$ 's will be the key.

However, no one knows how to iterate (32)-(33) as a black box, over time steps of length  $\tau$ . As we shall see in the next section, Deng, Hani and Ma solve this issue in a drastic way: they complement the ansatz with a *full* expansion of the  $E$ -functions, all the way from time zero up to arbitrary times, bounded by an *explicit* graph expansion (see Figure 13 and Sections 4.2, 4.4).

## 4. Long time derivation

### 4.1. The theorem by Deng, Hani, Ma

The breakthrough of Deng, Hani, and Ma (2024) is to extend Lanford's convergence result to much longer times than the mean free time. Note that this is not a simple technical extension of the previous proof since the series expansions (27) and (28) involving respectively  $\nu_\varepsilon$  and  $\tilde{\nu}_\varepsilon$  will be divergent, which is related to the fact that collision graphs on large time intervals  $[0, T]$  are expected to have giant components (see footnote (4)). The main challenge is then to find a way to combine:

- cluster expansions of the dynamics which converge only locally in time;
- the chaos assumption which is known to hold in a strong sense only at time 0.

Indeed (32) involves a  $L_v^1$  norm, in contrast with the assumptions at time zero which guarantee a similar estimate in  $L_v^\infty$ . The result (32) cannot be iterated as written, due to this loss in topology<sup>(7)</sup>.

The strategy implemented by Deng, Hani and Ma is therefore to design an iteration scheme which allows to extract at each time step the leading order terms (corresponding to a factorised state) and keep expanding only the remainders. The control on the leading order terms is then made possible due to a stability argument on the Boltzmann

---

<sup>(7)</sup>It is well known, since the work of Lanford, that the loss of topology is not merely a technical issue but rather an intrinsic feature of the low-density limit, inseparably linked to the transition to irreversibility discussed in Section 1.3.

equation, and requires as explained in Section 1.2 some regularity on its solution, which will be measured in the weighted space  $L_\beta^{\infty,1}$  defined by the following norm:

$$(34) \quad \|f\|_{L_\beta^{\infty,1}} := \sum_{k \in \mathbb{Z}^d} \sup_{|x-k| \leq 1} \sup_{v \in \mathbb{R}^d} \left| f(x, v) \exp\left(\frac{\beta}{2}|v|^2\right) \right|.$$

Their result can be stated as follows.

**THEOREM 4.1** (Deng, Hani, and Ma, 2024). — *In the low-density scaling (12),*

$$(35) \quad \lim_{\varepsilon \rightarrow 0} f_1^\varepsilon(t) = f(t)$$

*in  $L^1(\mathbb{R}^{2d})$ , for  $t$  in any finite time interval  $[0, T]$  such that the solution  $f$  to the Boltzmann equation with initial data  $f^0$  satisfies*

$$\forall t \in [0, T], \quad \|f(t)\|_{L_\beta^{\infty,1}} + \|\nabla_x f(t)\|_{L_\beta^{\infty,1}} \leq C$$

*for some  $C > 0$ ,  $\beta > 0$ .*

Note that, unlike Theorem 2.1, the convergence result (35) holds only in  $L^1(\mathbb{R}^{2d})$ .

**Remark 4.2** (On the functional setting). — The space  $L_\beta^{\infty,1}$  encodes both the exponential decay in  $v$ , and a decay at infinity in  $x$ . These properties ensure in particular that the total mass is finite, which is not the framework used to derive hydrodynamic limits of the Boltzmann equation (consisting in perturbations of the Maxwellian  $M_\beta$ ). In a recent preprint (Deng, Hani, and Ma, 2025), the authors derive an extension of Theorem 4.1 to the torus setting.

**Remark 4.3** (On diverging times). — Although the convergence result is stated on finite time intervals, the proof shows that it can be extended to slowly diverging times  $T_\varepsilon \rightarrow \infty$  as  $\varepsilon \rightarrow 0$  if the solution to the Boltzmann equation is global and satisfies

$$\sup_{t \in \mathbb{R}^+} \left( \|f(t)\|_{L_\beta^{\infty,1}} + \|\nabla_x f(t)\|_{L_\beta^{\infty,1}} \right) < +\infty.$$

Quantifying the divergence of  $T_\varepsilon$  is an important step to study fast relaxation limits leading to hydrodynamic models.

**Remark 4.4** (On the similarities with wave turbulence). — The proof of Theorem 4.1 shares many similarities with the derivation by the same authors of the wave kinetic equation from the weakly nonlinear Schrödinger equation <sup>(8)</sup> (Deng and Hani, 2023a, 2026, 2023b). Formal derivations of this equation date back to the early work of Peierls (1929) on phonons. A first rigorous result was obtained in (Lukkarinen and Spohn, 2011) in a close-to-equilibrium setting and for short times, using tools developed

<sup>(8)</sup>At the level of weakly nonlinear waves, the second moment of the wave field is governed by the wave kinetic equation, which is the counterpart of the Boltzmann equation. The analogue of the hard sphere empirical density is actually the so-called Wigner function, which is quadratic in the wave fields and random. In the kinetic limit, this object satisfies also a law of large numbers which is the counterpart of (15).

by Erdős, Salmhofer and Yau in the context of the linear Schrödinger equation with random potential (Erdős and Yau, 2000; Erdős, Salmhofer, and Yau, 2008). In their breakthrough series of papers, Deng and Hani were able to derive the nonlinear equation and they extended the result to arbitrarily long times. We refer to de Suzzoni (2025) for an introduction to these works which we will not comment further on as the setting is very different from the hard sphere dynamics, and we are not familiar enough with the details of the proof.

#### 4.2. Strategy of the proof

The strategy devised by Deng, Hani, and Ma (2024) is to establish a cumulant expansion of the correlation functions similar to (31) for further times  $T = \mathcal{L}\tau$ , where  $\mathcal{L}$  is an integer,

$$f_k^\varepsilon(\mathcal{L}\tau, \mathbf{z}_K) = \sum_{H \subset K} \left( f_1^\varepsilon \right)^{\otimes K \setminus H}(\mathcal{L}\tau) E_H^\varepsilon(\mathcal{L}\tau),$$

and to provide a graphical representation of the correlation errors  $E_H^\varepsilon(\mathcal{L}\tau)$  by iterating the dynamical cluster expansion (25) on the small time intervals  $[\ell\tau, (\ell+1)\tau]$ ,  $\ell < \mathcal{L}$ . The main difference between the dynamical cluster expansion on  $[0, \tau]$  and on any further time interval  $[\ell\tau, (\ell+1)\tau]$  is the fact that correlations at time  $\ell\tau$  are a priori no longer negligible : one has to keep track of the dynamical correlations on  $[0, \ell\tau]$ . In other words, the representation in Figure 11 where correlations come only from overlaps and collisions during the small time interval has to be changed to take into account previous correlations, meaning that on the bottom line some particles will be independent (represented by red bullets on the line  $t = \tau$  in Figure 12), while other will be already correlated (represented by purple bullets in Figure 12).

As already mentioned, iterating the whole cluster expansion on each time step would lead to divergent series (due to the huge number of graphs). Note that this divergence still holds when looking at the iterated expansion of the Boltzmann equation with Duhamel series. **The first key idea in the work by Deng, Hani and Ma is to extract the leading order terms which are factorised and should compare to the solution of the Boltzmann equation, and to expand only the correlation errors, for which the combinatorics of the graphs should be compensated by the smallness coming from the geometric constraints.** This idea of extracting the maximally factorised state is not present at all in the proof of Theorem 2.1, where propagation of chaos is obtained as a consequence of the convergence of the correlation functions to the Boltzmann hierarchy. It appeared in subsequent works when establishing more quantitative chaos estimates in (Pulvirenti and Simonella, 2017), or looking at fluctuations in (Bodineau, Gallagher, Saint-Raymond, and Simonella, 2023b). But, for hard spheres, it had not been implemented before to obtain information on the maximally factorised state thanks to the solution of the Boltzmann equation, and to improve the convergence.

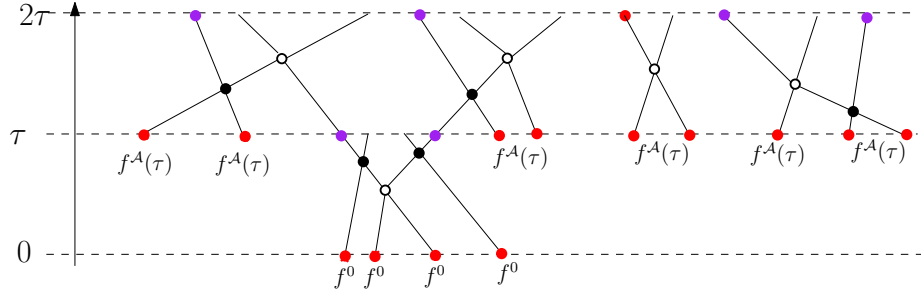


FIGURE 12. The collision graph depicted during the time interval  $[\tau, 2\tau]$  involves 11 particles at time  $\tau$ . It is a contribution to a term of the type  $f^A(2\tau)E_H^\varepsilon(2\tau)$  with  $|H| = 4$  in an expansion similar to (33). We have introduced here the notation  $f^A$ , used by Deng, Hani and Ma to indicate an approximation to the Boltzmann density. In the example of this figure,  $f_{11}^\varepsilon(\tau)$  is further expanded in a similar way and the purple particles in  $H_1$ , with  $|H_1| = 2$ , associated to the correlation error at time  $\tau$ . These particles are dynamically correlated in the past, whereas the particles indicated by red bullets at time  $\tau$  are independently distributed and for those particles we stop the expansion. The error function  $E_{H_1}^\varepsilon(\tau)$  is computed by another expansion on  $[0, \tau]$  with the conditions that the particles in  $H_1$  interact dynamically. For simplicity the initial measure is chosen to be a product (neglecting the initial correlations which are much smaller than the dynamical correlations).

Let us describe the strategy in a little more detail. Set  $s \geq 1$ . To identify the different correlation errors in  $f_s^\varepsilon((\ell + 1)\tau, \mathbf{z}_s)$ , one argues iteratively. One first applies the cluster expansion (25) in  $[\ell\tau, (\ell + 1)\tau]$  and then evaluates it by using the representation (31) of  $(f_{K_\ell}^\varepsilon(\ell\tau))_{K_\ell}$  according to the following rules (we have added subscripts  $\ell$  to the sets  $H$  and  $K$  to emphasize that the study takes place on the time step  $[\ell\tau, (\ell + 1)\tau]$ ):

1. the variables in  $K_\ell \setminus H_\ell$  are integrated with respect to the density  $f_1^\varepsilon(\ell\tau)$  which is close to  $f(\ell\tau)$  by the induction assumption,
2. the variables in  $H_\ell$  are called *root particles* and they are dynamically correlated in the past history in  $[0, \ell\tau]$ . Thus another cluster expansion in the previous time interval is needed to compute their joint distribution.

The previous simple extraction is actually not sufficient to control the expansion of the correlation errors. Indeed the previous short time cluster expansion (25) leads to collision graphs which can be a priori arbitrarily large and have an unbounded number of recollisions. Both events are very unlikely and have been neglected in the time interval  $[0, \tau]$  to derive the convergence to the Boltzmann equation (see Section 3). For the iteration, it is convenient to remove these events from the main part by introducing *truncated microscopic dynamics*<sup>(9)</sup>, and deriving a modified cumulant expansion of type (33) involving an error term, obtained by a modified Penrose argument<sup>(10)</sup>.

<sup>(9)</sup>Section 4.1 in Deng, Hani, and Ma (2024).

<sup>(10)</sup>Section 5 in Deng, Hani, and Ma (2024).

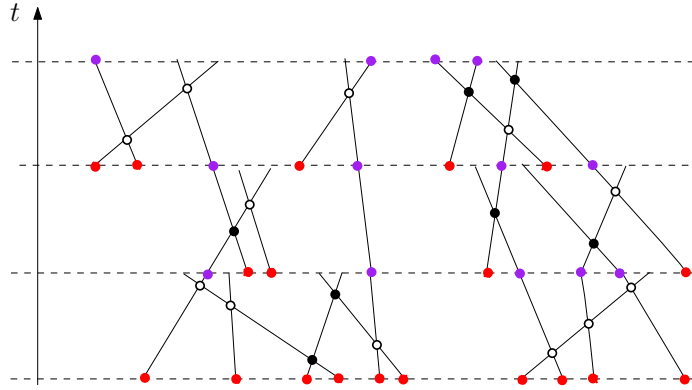


FIGURE 13. Three time layers representing a correlation term  $E_H(3\tau)$  between  $|H| = 4$  root particles at time  $3\tau$ . The dynamical correlations between the root particles form cycles which may spread over several layers.

To reach a large time  $T = \mathcal{L}\tau$ , the previous strategy is iterated thanks to a *time layering* procedure<sup>(11)</sup> (see Figure 13). Applying the rules above at each step, one gets the general version of (33)

$$(36) \quad f_k^\varepsilon(\ell\tau, \mathbf{z}_K) = \sum_{H \subset K} (f^A)^{\otimes K \setminus H}(\ell\tau) E_H^\varepsilon(\ell\tau) + \text{Err}^\varepsilon(\ell\tau, \mathbf{z}_K),$$

where

1.  $f^A(\ell\tau)$  is similar to  $f(\ell\tau)$  but is a better approximation of  $f_1^\varepsilon(\ell\tau)$ , and is built on the truncated dynamics. This means that, on each layer, each collision graph has size less than a certain threshold  $\Lambda$  and has less than a fixed number  $\Gamma$  recollisions. Furthermore the number of overlaps in each cluster (or molecule with the terminology of Deng, Hani and Ma) cannot exceed  $\Lambda$ . The cut-off  $\Lambda \leq |\log \varepsilon|^{C_0^*}$ , for  $C_0^*$  a given constant is allowed to diverge slowly, instead  $\Gamma$  will be chosen large but fixed.
2. The correlation error  $E_H^\varepsilon$  is obtained by a cluster expansion and also built on the truncated dynamics.
3. The error  $\text{Err}^\varepsilon$  collects all the remainders accumulating at all steps and will converge to zero with  $\varepsilon$  in  $L^1$ -norm.

The distribution  $f^A(\ell\tau)$  is approximated step by step by the solution of the Boltzmann equation. In particular it is shown<sup>(12)</sup> that

$$(37) \quad \|f^A(\ell\tau) - f(\ell\tau)\|_{L_{\beta_\ell}^{\infty,1}} \leq \varepsilon^{\theta_\ell}$$

for some  $\beta_\ell > 0$  and  $\theta_\ell > 0$  that can be explicitly computed<sup>(13)</sup>. The existence of a regular solution to the Boltzmann equation on the time interval  $[0, T]$  is key to establish

<sup>(11)</sup>Proposition 3.25 in Deng, Hani, and Ma (2024).

<sup>(12)</sup>Proposition 6.1, proved in Section 14 in (Deng, Hani, and Ma, 2024).

<sup>(13)</sup>(1.34) in (Deng, Hani, and Ma, 2024).

this estimate, see Section 4.3 below. Besides the existence of such a solution, the proof of Deng, Hani and Ma does not use any other mechanism of cancellation in the Boltzmann equation.

The dynamical correlations are shown to be negligible due to the constraint on the recollisions<sup>(14)</sup>:

$$(38) \quad \|E_H^\varepsilon(\ell\tau)\|_{L^1} \leq \varepsilon^{3^{-d-2} + c^*|H|},$$

where  $|H|$  stands for the number of particles in  $H$ . Roughly speaking each root particle at time  $\mathcal{L}\tau$  (depicted in purple on Figure 13) is correlated with at least one other root particle and the corresponding dynamical constraints provide a small factor of order  $\varepsilon^\rho$ . As can be seen on Figure 13, this correlation can appear through several layers and many other root particles can be generated in the iterative procedure. The cut-off  $\Lambda \leq |\log \varepsilon|^{C_0^*}$  on the size of the molecules (clusters) is needed to tame the combinatorial factor on the number of all molecules (see condition (2) in the description below (36), and Section 4.4 below for more). Nevertheless the number of allowed recollisions can lead to a huge complexity of dynamical patterns. The analysis of the recollisions is the main achievement of the proof by Deng, Hani and Ma, and is based on a precise algorithmic decomposition of the collision graphs, see Section 4.4 below.

### 4.3. The maximally factorised part

By construction, the distribution  $f^A((\ell + 1)\tau)$  (which is represented by red circles on Figure 12 and subsequent figures) is defined recursively by a dynamical cluster expansion on  $[\ell\tau, (\ell + 1)\tau]$

- such that each collision graph has size less than  $\Lambda$  and has less than  $\Gamma$  recollisions, and the number of overlaps in the cluster is less than  $\Lambda$ ,
- acting on independent particles distributed according to  $f^A(\ell\tau)$ .

On the other hand, the solution  $f((\ell + 1)\tau)$  to the Boltzmann equation can be represented by a dynamical cluster expansion on  $[\ell\tau, (\ell + 1)\tau]$

- such that each cluster is a binary tree graph,
- acting on independent particles distributed according to  $f(\ell\tau)$ .

In order to compare both distributions, the idea is to further decompose

$$(39) \quad f^{\mathcal{A}} = \bar{f}^{\mathcal{A}} + \delta f^{\mathcal{A}}$$

where the leading term  $\bar{f}^{\mathcal{A}}$  corresponds to the restriction to (bounded) clusters which are minimally connected, and

$$(40) \quad f = \bar{f} + \delta f$$

where the leading term  $\bar{f}$  corresponds to the restriction to (minimally connected) clusters which have size less than  $\Lambda$ .

<sup>(14)</sup>Proposition 6.2 in Deng, Hani, and Ma (2024).

The difference  $\bar{f}^A - \bar{f}$  is controlled using a kind of **weak-strong stability principle for the Boltzmann equation in mild form**. The cancellation exhibited in Figure 10 (Step (3) of the proof of Lanford's theorem described on page 19) shows that the tree graphs involved in the definition of  $\bar{f}^A((\ell+1)\tau)$  can be reduced to binary tree graphs. In other words,  $\bar{f}^A((\ell+1)\tau)$  and  $\bar{f}((\ell+1)\tau)$  have the same cluster expansion, acting respectively on  $\bar{f}^A(\ell\tau)$  and  $\bar{f}(\ell\tau)$ , and with a small spatial discrepancy due to the  $\varepsilon$  distance separating collisional particles in  $\bar{f}^A(\ell\tau)$  contrary to  $\bar{f}(\ell\tau)$ .

Using the multilinearity of the cluster expansion, we then obtain that each single term in the sum defining  $(\bar{f}^A - \bar{f})((\ell+1)\tau)$  has at least one occurrence of  $(\bar{f}^A - \bar{f})(\ell\tau)$  or one occurrence of  $\varepsilon \nabla_x f(\ell\tau)$ , which allows to propagate the smallness (up to a small loss due to the contribution of large velocities) from time  $\ell\tau$  to time  $(\ell+1)\tau$ .

The contribution  $\delta f$  in (40) is easily shown to be small, as the remainder of a geometric series (recall that the time-step is  $\tau$  only, so the series is under control). The contribution  $\delta f^A$  of the subleading terms in  $f^A$  in (39) requires much more care because of the need to compensate the loss due to large velocities. This loss is more or less proportional to the size of the molecule, i.e. to the total number of collisions and overlaps which can be much bigger than the number of particles in the cluster. One thus needs to gain additional smallness, which comes from the geometric constraints associated to the recollisions. This is done thanks to a simplified version of the algorithms used to control correlation errors sketched in the section below.

#### 4.4. The remainder terms

The core of the paper by Deng, Hani, and Ma (2024) is the estimate (38) of the remainder term which takes into account the recollisions. Recall that the time interval  $[0, T]$  is split into  $\mathcal{L}$  layers of size  $\tau$ . As explained in Section 4.2, given  $\ell \leq \mathcal{L}$ , the remainder term  $E_H^\varepsilon(\ell\tau, \mathbf{z}_H)$  at time  $\ell\tau$  can be estimated in  $L^1$  by computing, for all compatible molecules  $\mathbb{M}$ , the cost (smallness) of the constraint that the root particles (recall they are the particles in  $H$ , represented by purple bullets) have to be correlated, as in Figure 13. A similar combinatorial classification of correlation terms has been previously developed in the context of wave turbulence to derive the wave kinetic equation from the (microscopic) nonlinear Schrödinger equation; see Deng and Hani (2023b) and references therein.

The cost of a molecule is an upper bound on the concatenation of the cluster expansion weights associated with  $\mathbb{M}$  over  $\ell$  layers. A molecule  $\mathbb{M}$  is interpreted as a graph such that a collision or an overlap is coded by a node and the edges are particle trajectories between 2 nodes. These nodes have degree 4 (2 incoming and 2 outgoing particles) and if a particle trajectory stops, or is created between two layers, the corresponding node has degree 1 (represented respectively by free ends or by red dots in Figure 13).

Let us first estimate the combinatorics of molecules. The number of graphs with degree less than 4, with  $m$  nodes and  $\rho$  independent cycles, is bounded by  $C^m m^\rho$ .

Roughly, there are less than  $C^m$  trees and each cycle boils down to adding a link between two nodes. Given  $m \leq |\log \varepsilon|^{C_0^*}$ , the number of molecules is estimated by

$$(41) \quad \#\{\mathbb{M}, |\mathbb{M}| = m, \rho \text{ cycles}\} \leq C^m m^\rho \leq C^m |\log \varepsilon|^{C_0^* \rho}.$$

The logarithmic bound on the molecule size was imposed in the construction of each time layer (see condition (2) below (36)). This is essential to control the combinatorics, and the additional error term  $\text{Err}^\varepsilon$  in (36) takes this cut-off into account.

The divergence in the combinatorial factor (41) has to be compensated by the cost of the recollisions associated with the molecules involved in  $E_H^\varepsilon$ . On a single time layer, we have already seen that one single recollision is enough to provide some smallness and to derive the chaos property (30). More generally quantitative bounds on the correlations of  $j$  particles were stated in (32). The bound provided in (Deng, Hani, and Ma, 2024) on each given molecule is much stronger: not only does it hold on a large time since  $\ell$  is arbitrary, but it provides additional smallness for each cycle. We will concentrate here on the difficult case when the number  $\rho$  of cycles can be much larger than the cardinality of  $|H|$ . **The major breakthrough by Deng, Hani and Ma<sup>(15)</sup> is to establish that there is  $\gamma > 0$  such that the cost of a given molecule can be estimated by  $\tau^{|\mathbb{M}|/9} \varepsilon^{\gamma \rho}$ , meaning that the gain in smallness on the cost of the molecule is proportional to the number  $\rho$  of cycles.** The upper bound (38) on  $\|E_H^\varepsilon(\ell\tau)\|_{L^1}$  follows by combining (41) and this upper bound.

Given a molecule  $\mathbb{M}$ , computing its cost can be seen as evaluating an integral over the parameters associated with the trajectories compatible with  $\mathbb{M}$ . In the proof by Deng, Hani and Ma<sup>(16)</sup>, the molecules are overparametrised as each collision/overlap is determined by  $8d + 1$  variables : one for the position and velocity on each of the 4 edges and one for the time of the collision/overlap. Thus a given particle is associated with several sets of distinct variables strongly correlated by the constraints at each collision/overlap. The range of these parameters is further reduced by the dynamical constraints of the cycles imposed by  $\mathbb{M}$  so that the smallness follows from the integration over the trajectory parameters (see Figure 14). The idea behind the duplication of the integration variables is to forget the original structure of the trajectories and to compute the multiple integrals in any order provided the dynamical constraints are satisfied. For example, the position and velocity of a particle can be chosen at the beginning of a time layer or in the middle of it. The difficulty is to **determine, among all these variables, which are the degrees of freedom providing the best parametrisation of (a large proportion of) the cycles<sup>(17)</sup>**. Ordering the parameters will be achieved by an algorithmic procedure described below. Once an order is determined, one can use a Fubini argument to control the cost of the molecule.

<sup>(15)</sup>Eq. (9.53) of their paper, up to some terms which have been omitted for simplicity.

<sup>(16)</sup>Definition 7.3.

<sup>(17)</sup> This problem has an analogue in the derivation of wave kinetic equations and the strategy is inspired from previous literature on this topic; see Deng and Hani (2023b) and references therein.

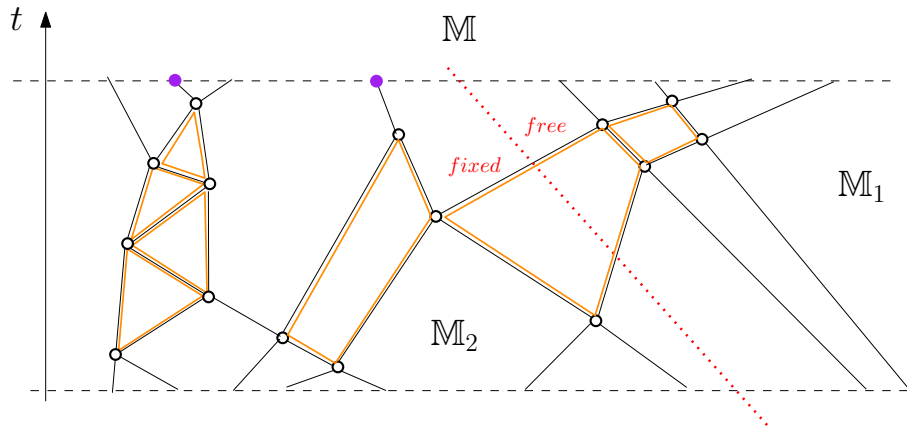


FIGURE 14. In this figure, the graph represents a molecule  $M$  with several cycles and  $H$  is of size 2. On the left a chain of collisions between a small number of particles creates several cycles. The constraints imposed by a molecule  $M$  with cycles imply that the parameters of the trajectories take values in a very small set of the phase space. The challenge is to identify the degrees of freedom among these parameters in order to gain a power  $\varepsilon^{\gamma\rho}$  proportional to the number of cycles  $\rho$ . This is done by splitting the molecule  $M$  into smaller entities on which the integration can be performed step by step. For example, the dotted line decomposes the molecule  $M$  into 2 molecules  $M_1, M_2$  which will be evaluated one after the other. Given a configuration in  $M_1$ , the particle trajectories crossing the dotted line are frozen and one has to integrate first over the degrees of freedom restricted to  $M_2$  to obtain estimates on the cycles uniformly in  $M_1$  and then to integrate over the parameters in  $M_1$ . A complete splitting procedure is depicted on Figure 16.

As can be imagined from Figure 14, the cycles associated with a molecule can be extremely intricate, leading to long range constraints on the parameters. In particular forcing a cycle to occur may trigger several cycles in chain reaction, in which case one cannot hope to gain easily a factor  $\varepsilon^c$  each time (see also Figure 17). The strategy devised by Deng, Hani and Ma identifies the degrees of freedom by **decomposing the molecules through several algorithmic procedures**<sup>(18)</sup> in order to reduce the complexity of dynamical graphs to elementary molecules<sup>(19)</sup> as in Figure 15 involving only a few parameters. The elementary molecules are made of one or two collisions or overlaps (called *atoms* by Deng, Hani and Ma). The nature of the elementary molecules is determined by the number of degrees of freedom and they are classified into 3 categories: *normal*, *good* and *bad*<sup>(20)</sup>. Molecules {3} (and sometimes {2}) are the basic elements in the complex molecules and they can be estimated by constants. The dynamical constraints of the cycles are encoded by the {33}-molecules which have a

<sup>(18)</sup>Sections 10 to 12 in (Deng, Hani, and Ma, 2024).

<sup>(19)</sup>Definition 8.11 in (Deng, Hani, and Ma, 2024).

<sup>(20)</sup>See Definition 9.4 of Deng, Hani, and Ma (2024) for the precise description of the 11 categories.

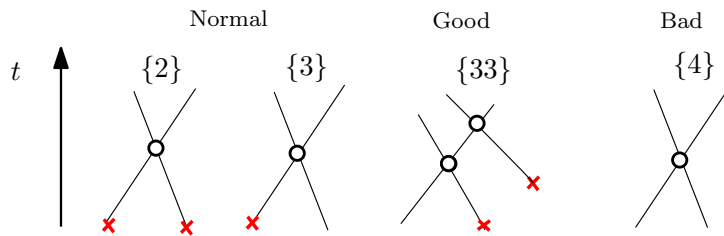


FIGURE 15. Some of the elementary molecules are represented above (see Definition 8.11 of Deng, Hani, and Ma (2024)). The crosses represent variables which are given (or fixed). A  $\{2\}$ -molecule has 2 incoming fixed edges and therefore the outgoing particle trajectories are fully determined. A  $\{3\}$ -molecule has only 1 incoming fixed edge and the other incoming edge provides a degree of freedom which can act on the outgoing edges. A  $\{33\}$ -molecule encodes the cost of a recollision. Indeed the single incoming (free) edge (at the bottom) is strongly constrained as the outgoing particle of the first collision has to collide with the 2nd fixed particle trajectory. Integrating over this constraint leads to a small  $\varepsilon^c$  factor and in this sense  $\{33\}$  are good molecules. Finally, the  $\{4\}$ -molecule has no constraint and is considered as bad because integrating over too many degrees of freedom leads to a loss. Similar elementary molecules can be considered by fixing the outgoing parameters instead or by replacing the collisions by overlaps.

cost of  $\varepsilon^c$  (see Figure 15). Thus  $\{2\}$  and  $\{3\}$ -molecules are said to be *normal* and  $\{33\}$ -molecules are *good*. Molecules  $\{4\}$  are *bad* since all variables are free, and the geometric constraint associated to the collision or overlap is not taken into account. Note that bad molecules may appear during the decomposition leading to losses which have to be compensated by enough gains with the  $\{33\}$  molecules. The precise cost of the elementary molecules is evaluated by computing collision integrals depending only on a few parameters<sup>(21)</sup>.

The decomposition of a molecule  $\mathbb{M}$  into elementary molecules  $\{2\}$ ,  $\{3\}$ ,  $\{33\}$  and  $\{4\}$  is achieved in many steps starting from the large scales (see Figure 14) to localise progressively the costly structures of the cycles. In Figure 16 below, an example of a single cycle decomposition is depicted, following the **UP algorithm**<sup>(22)</sup>. It is the simplest algorithm of a series of procedures in order to analyse the numerous structures which can arise in the molecules. But it is not enough to gain a power of  $\varepsilon^c$  for each cycle when the cycles in a molecule are very intricate, as in Figure 17.

<sup>(21)</sup>Section 9 in (Deng, Hani, and Ma, 2024).

<sup>(22)</sup>Definition 12.1 in (Deng, Hani, and Ma, 2024).

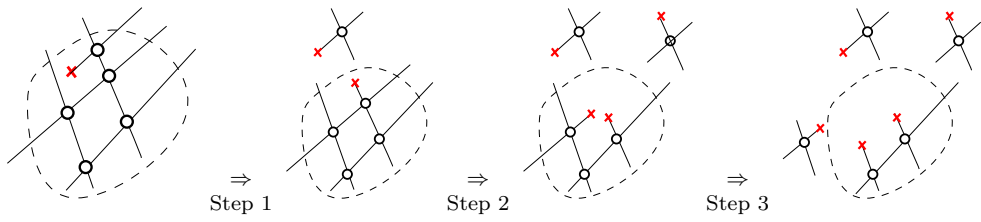


FIGURE 16. On the left, a molecule involving a cycle is depicted and the edges outside the dashed domain have not been explored yet by the algorithms. In the UP algorithm, the atoms are removed one after the other starting from the top collision in order to keep track of the time ordering associated with the molecule. In the first step, the top atom has been extracted as a  $\{3\}$ -molecule, meaning that the remaining edge in the dashed domain is now considered fixed. After the final step, three elementary  $\{3\}$ -molecules have been identified and a  $\{33\}$ -molecule will lead to a small cost  $\varepsilon^c$ . In this example, one cycle provides exactly one  $\{33\}$ -molecule as expected. For general molecules with overlaps, the decomposition procedure is more delicate as breaking an overlap may lead to non local changes.

Recall that in (36), the main term of the cluster expansion has been devised so that, in each layer, a cluster has less than  $\Gamma$  recollisions. Under this condition, the succession of recollisions between a finite number of particles, as in Figure 17, is no longer a problem as the number of recollisions is bounded by  $\Gamma$ . Thus extracting a single power  $\varepsilon^c$  is enough to take into account the cycles due to recollisions within a cluster in a given layer, with a cost of  $\varepsilon^{c/\Gamma}$  per cycle.

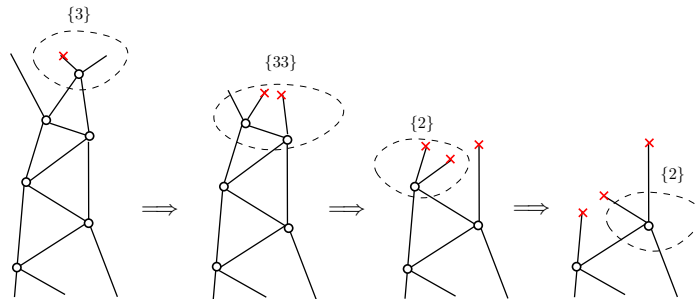


FIGURE 17. A series of cycles obtained by multiple recollisions of 3 particles is depicted on the left (see Figure 14). The UP algorithm is applied to the corresponding molecule, starting from the top, in order to decompose it into elementary molecules. After removing the top  $\{3\}$ -molecule, a  $\{33\}$ -molecule is extracted in the second step from the first cycle. This exhausts all the degrees of freedoms and the next steps will only form  $\{2\}$ -molecules. Indeed fixing 2 outgoing edges of a collision prescribes exactly the 2 incoming edges and this constraints propagate along the chain of cycles. Thus only the first constraint can be extracted from this series of recollisions and the gain will not be proportional to the number of cycles.

However this condition does not prevent the **occurrence of an arbitrary number of strongly correlated cycles formed through different layers**. There are four main structures of two-layer molecules of this type, named *toy models*<sup>(23)</sup> (see Figure 18 for an example of the first toy model). Each toy model is specific and different algorithms are needed in each case to identify degrees of freedom<sup>(24)</sup>. The toy models have a very streamlined structure : roughly speaking they look like two trees on each side of a layer with leaves glued together to form cycles.

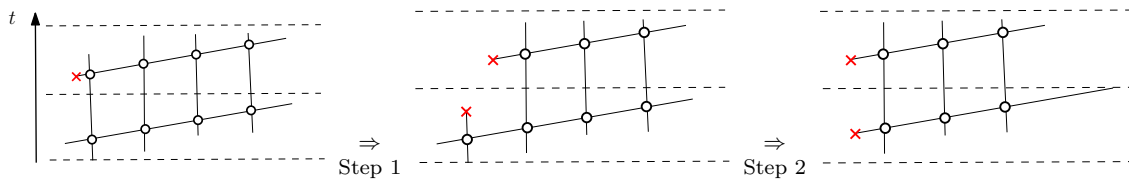


FIGURE 18. The left figure depicts a chain of cycles with a ladder structure across two layers represented by dashed lines. After removing the first two nodes on the left (as  $\{3\}$ -molecules), one gets a  $\{33\}$ -molecule for each step of the ladder. This leads to a gain  $\varepsilon^{c\rho}$  proportional to the length of the ladder, i.e. to the number of cycles  $\rho$ . Note that the order in which the atoms are removed is key and a different procedure could have led only to a gain of order  $\varepsilon^c$ .

A general molecule  $\mathbb{M}$  is a priori much more complicated and does not have this tree-like structure. In fact the cycles can spread over several layers and not necessarily over two contiguous layers as in Figure 18. Given a molecule  $\mathbb{M}$ , an essential part of the proof<sup>(25)</sup> is to clean up  $\mathbb{M}$  in order to retain only the basic form of a toy model and discard (in a controlled way) the rest of the molecule. This goes through a series of delicate procedures among which the most important are:

1. Removing the degeneracies in positions and velocities<sup>(26)</sup>;
2. Reducing the molecule in each layer to a tree by fragmenting each layer;
3. Selecting the two layers across which most of the cycles will form;
4. Cutting exceptional components.

Combining all the previous procedures allows one to select the degrees of freedom associated with a large proportion of the cycles in a molecule.

<sup>(23)</sup>Section 11 in (Deng, Hani, and Ma, 2024).

<sup>(24)</sup>We refer to Section 11 of Deng, Hani, and Ma (2024) for an overview of those and to Section 13 for the complete implementation.

<sup>(25)</sup>Section 12 in (Deng, Hani, and Ma, 2024).

<sup>(26)</sup>For some particle configurations, a recollision may occur with high probability, e.g. when 3 particles are initially close to each other. The corresponding  $\{33\}$ -molecules are said to be degenerate and they will not provide the expected gain of order  $\varepsilon^c$ . The occurrence of too many such events has to be estimated by other means.

*Remark 4.5.* — To handle the remainder term in (36) corresponding to clusters with more than  $\Gamma$  recollisions, a new algorithm had to be devised<sup>(27)</sup>. The key idea is to use a weak form of dispersion in  $\mathbb{R}^d$  provided by the following quantitative statement by Burago, Ferleger, and Kononenko (1998) : any collection of  $q$  hard spheres in  $\mathbb{R}^d$  will recollide at most  $O(q^{q^2})$  times. Even though this estimate is far too crude in general, it provides a universal bound, so that if the number of recollisions between  $q$  hard spheres is too large, there must be an additional particle involved in the cycles and therefore a new degree of freedom. The use of this dispersion argument is the reason why the proof does not extend directly to the case of a hard-sphere gas in the torus  $\mathbb{T}^d$ .

## 5. Consequences and perspectives

The paper by Deng, Hani, and Ma (2024) is a crucial advance in deriving macroscopic laws rigorously from microscopic models using the Boltzmann equation as an intermediate description, which was one of the questions addressed by Hilbert in his sixth problem. Hydrodynamic models such as the compressible Euler equations, or the incompressible Navier–Stokes equations can indeed be recovered as asymptotics of the Boltzmann equation in the fast relaxation limit, i.e. when the collision process is much faster than the transport. In order to complete the program and make a connection with particle systems, one therefore needs to derive the Boltzmann equation for times which are much longer than the mean free time.

As mentioned in Remark 4.2, although it provides a convergence for times which are much longer than the mean free time, Theorem 4.1 is not exactly the result we need, because the functional setting imposed by (34) prevents us from considering initial distributions which are fluctuations around an equilibrium or satisfy at least a bound from below on the macroscopic density, which is required for all hydrodynamic limits. Furthermore, as noted in Remark 4.3, Theorem 4.1 does not provide a quantitative estimate on the time of validity of the Boltzmann approximation, which would be necessary to make explicit the scaling laws leading to the hydrodynamic limits from the particle system via the Boltzmann approximation.

The recent preprint by Deng, Hani, and Ma (2025) aims at addressing these two objections. It relies on a similar proof, where the use of Burago, Ferleger, and Kononenko (1998) is adapted with a new cutting algorithm. It states the convergence from the hard-sphere dynamics to the compressible Euler equations, and incompressible Navier–Stokes equations, under strong regularity assumptions (which are known to be violated in the presence of compressible shocks for instance).

It is worth stressing that the direct hydrodynamic limit from Hamiltonian particle systems, with no smallness in the density, is far from being understood and involves different kinds of problems. This limit should lead to the Euler and the Navier–Stokes

---

<sup>(27)</sup>Section 15 of Deng, Hani, and Ma (2024).

equations for real fluids<sup>(28)</sup>. At present, a full mathematical result has been obtained only for stochastic dynamics (see Olla, Varadhan, and Yau, 1993; Esposito, Marra, and Yau, 1996).

A natural question would be to know whether the techniques in (Deng, Hani, and Ma, 2024) can be extended to handle the fluctuations and large deviations both at the kinetic level and at the hydrodynamic level. Using refined cluster expansions (where the correlation error is further decomposed in cumulants corresponding to connected interaction graphs), we have proved in (Bodineau, Gallagher, Saint-Raymond, and Simonella, 2023b) that, in the low-density limit, fluctuations of the hard-sphere dynamics around the Boltzmann approximation can be described by the fluctuating Boltzmann equation, and large deviations can be described by a functional which satisfies some Hamilton-Jacobi equation. However, like Lanford’s theorem, these results hold only for short times (except at equilibrium where both the linear fluctuating Boltzmann equation, and the linear fluctuating Stokes-Fourier equations are derived globally in time in (Bodineau, Gallagher, Saint-Raymond, and Simonella, 2024b) and (Bodineau, Gallagher, Saint-Raymond, and Simonella, 2024a)). It has recently been proved by Qi (2024) that the Hamilton-Jacobi equations are globally well-posed close to equilibrium, so one can hope to push the techniques of Deng, Hani, and Ma (2024) to that setting.

Another important problem, which remains fully open in the field, is the low-density limit of microscopic systems in which the interaction potential is not compactly supported, which is more relevant from the physical point of view (for some first partial results in this direction, see Ayi, 2017, and Le Bihan, 2025b). The main difficulty in this case is that the cross section (encoding the rate of the jump process  $(v', v'_*, \omega) \mapsto (v, v_*, \omega)$  in the Boltzmann collision operator) is not integrable. In particular, the gain and loss terms do not converge separately, and cancellations have to be used to make sense of the equation. A natural question is whether this type of cancellations could be exploited indirectly by assuming the existence of a regular solution, as in the argument by Deng, Hani and Ma presented in Section 4, to obtain a stable control of the microscopic dynamics.

## References

R. Alexander (1976). “Time Evolution for Infinitely Many Hard Spheres”, *Commun. in Math. Phys.* **49**, pp. 217–232.

N. Ayi (2017). “From Newton’s law to the linear Boltzmann equation without cut-off”, *Comm. Math. Phys.* **350** (3), pp. 1219–1274.

---

<sup>(28)</sup>For a recent discussion on the comparison of the different limit procedures, see e.g. Pulvirenti and Simonella (2026).

H. van Beijeren, O. E. Lanford III, J. Lebowitz, and H. Spohn (1980). “Equilibrium Time Correlation Functions in the Low-Density Limit”, *Journal Stat. Phys.* **22** (2), pp. 237–257.

T. Bodineau, I. Gallagher, and L. Saint-Raymond (2016). “The Brownian motion as the limit of a deterministic system of hard-spheres”, *Inventiones mathematicae* **203** (2), pp. 493–553.

T. Bodineau, T. Gallagher, L. Saint-Raymond, and S. Simonella (2020). “Fluctuation theory in the Boltzmann-Grad limit”, *J. Stat. Phys.* **180** (1-6), pp. 873–895.

——— (2022). “Cluster expansion for a dilute hard sphere gas dynamics”, *J. Math. Phys.* **63** (7), Paper No. 073301, 26 pp.

——— (2023a). “Long-Time Correlations for a Hard-Sphere Gas at Equilibrium”, *Comm. Pure Appl. Math.* **76** (12), pp. 3852–3911.

——— (2023b). “Statistical dynamics of a hard sphere gas: fluctuating Boltzmann equation and large deviations”, *Ann. of Math. (2)* **198** (3), pp. 1047–1201.

——— (2024a). “Dynamics of Dilute Gases at Equilibrium: From the Atomistic Description to Fluctuating Hydrodynamics”, *Ann. Henri Poincaré* **25**, pp. 213–234.

——— (2024b). “Long-time derivation at equilibrium of the fluctuating Boltzmann equation”, *Ann. Probab.* **52** (1), pp. 217–295.

D. Burago, S. Ferleger, and A. Kononenko (1998). “Uniform estimates on the number of collisions in semi-dispersing billiards”, *Ann. Math. (2)* **147** (3), pp. 695–708.

S. Caprino, A. De Masi, E. Presutti, and M. Pulvirenti (1991). “A derivation of the Broadwell equation”, *Comm. Math. Phys.* **135** (3), pp. 443–465.

T. Carleman (1932). “Sur la théorie de l'équation intégrérodifférentielle de Boltzmann”, *Acta Math.* **60**, pp. 369–424.

N. Catapano (2018). “The rigorous derivation of the Linear Landau equation from a particle system in a weak-coupling limit”, *Kin. Rel. Mod.* **11** (3), pp. 647–695.

C. Cercignani (1972). “On the Boltzmann equation for rigid spheres”, *Transport Theory Statist. Phys.* **Vol. 2**, pp. 211–225.

——— (1998). *Ludwig Boltzmann. The man who trusted atoms*. Oxford: Oxford University Press.

C. Cercignani, V. I. Gerasimenko, and D. I. Petrina (1997). *Many-Particle Dynamics and Kinetic Equations*. Kluwer Academic Publishers, Netherlands.

C. Cercignani, R. Illner, and M. Pulvirenti (1994). *The mathematical theory of dilute gases*. Vol. 106. Applied Mathematical Sciences. Springer-Verlag, New York, pp. viii+347.

A. De Masi and E. Presutti (1991). *Mathematical methods for hydrodynamic limits*. Vol. 1501. Lecture Notes in Mathematics. Springer-Verlag, Berlin, pp. x+196.

Y. Deng and Z. Hani (2023a). “Full derivation of the wave kinetic equation”, *Invent. Math.* **233** (2), pp. 543–724.

——— (2023b). *Long time justification of wave turbulence theory*. arXiv: [2311.10082](https://arxiv.org/abs/2311.10082).

——— (2026). “Derivation of the wave kinetic equation: full range of scaling laws.” *Mem. Amer. Math. Soc.* To appear.

Y. Deng, Z. Hani, and X. Ma (2024). *Long time derivation of the Boltzmann equation from hard sphere dynamics*. arXiv: [2408.07818v3](https://arxiv.org/abs/2408.07818v3).

——— (2025). *Hilbert’s sixth problem: derivation of fluid equations via Boltzmann’s kinetic theory*. arXiv: [2503.01800](https://arxiv.org/abs/2503.01800).

R. Denlinger (2018). “The propagation of chaos for a rarefied gas of hard spheres in the whole space”, *Arch. Ration. Mech. Anal.* **229** (2), pp. 885–952.

R. J. DiPerna and P.-L. Lions (1989). “On the Cauchy problem for Boltzmann equations: global existence and weak stability”, *Ann. of Math.* (2) **130** (2), pp. 321–366.

T. Dolmaire (2023). “About Lanford’s theorem in the half-space with specular reflection”, *Kin. Rel. Mod.* **16** (2), pp. 207–268.

L. Erdős, M. Salmhofer, and H. T. Yau (2008). “Quantum diffusion of the random Schrödinger evolution in the scaling limit I. The non-reollision diagrams.” *Acta Math.* **200** (2), pp. 211–277.

L. Erdős and H. T. Yau (2000). “Linear Boltzmann equation as the weak coupling limit of a random Schrödinger equation”, *Commun. Pure Appl. Math.* **53** (6), pp. 667–735.

R. Esposito, R. Marra, and H. T. Yau (1996). “Navier-Stokes equations for stochastic particle systems on the lattice”, *Commun. Math. Phys.* **182** (2), pp. 395–455.

F. Fougères (2024). “On the derivation of the linear Boltzmann equation from the nonideal Rayleigh gas”, *J. Stat. Phys.* **191** (10), Paper No. 136, 16 pp.

I. Gallagher, L. Saint-Raymond, and B. Texier (2014). *From Newton to Boltzmann: hard spheres and short-range potentials*. Zurich Lect. in Adv. Math. EMS.

V. I. Gerasimenko and I.V. Gapyak (2021). “Boltzmann-Grad asymptotic behavior of collisional dynamics”, *Rev. Math. Phys.* **33** (2). Article N. 2130001, 32 p.

H. Grad (1958). “Principles of the kinetic theory of gases”, in: *Handbuch der Physik*. Springer-Verlag, Berlin-Göttingen-Heidelberg, pp. 205–294.

R. Illner and M. Pulvirenti (1989). “Global validity of the Boltzmann equation for two- and three-dimensional rare gas in vacuum: Erratum and improved result”, *Commun. Math. Phys.* **121** (1), pp. 143–146.

O. E. Lanford III (1975). “Time evolution of large classical systems”, in: *Dynamical systems, theory and applications (Rencontres, Battelle Res. Inst., Seattle, Wash., 1974)*. Vol. 38. Lecture Notes in Phys. Springer, Berlin-New York, pp. 1–111.

——— (1976). “On a derivation of the Boltzmann equation”, *Astérisque* **40**, pp. 117–137.

C. Le Bihan (2022). “Boltzmann-Grad limit of a hard sphere system in a box with diffusive boundary conditions”, *Disc. Cont. Dyn. Syst.* **42** (4), pp. 1903–1932.

——— (2025a). “Long time validity of the linearized Boltzmann equation for hard spheres: a proof without billiard theory”, *Arch. Ration. Mech. Anal.* **249** (4), Paper No. 40, 72 pp.

C. Le Bihan (2025b). *Long time validity of the linearized Boltzmann uncut-off and the linearized Landau equations from the Newton Law*. arXiv:2408.03597.

J. Loschmidt (1876). *Sitzungsberichte der Kaiserlichen Akademie der Wissenschaften Wien, Math. Naturwiss. Klasse* **73**, pp. 128–142.

J. Lukkarinen and H. Spohn (2011). “Weakly nonlinear Schrödinger equation with random initial data”, *Invent. Math.* **183**, pp. 79–188.

K. Matthies and F. Theil (2012). “A semigroup approach to the justification of kinetic theory”, *SIAM J. Math. Anal.* **44** (6), pp. 4345–4379.

L. Nirenberg (1972). “An abstract form of the nonlinear Cauchy-Kowalewski theorem”, *Jour. Diff. Geom.* **6**, pp. 561–576.

S. Olla, S.R.S. Varadhan, and H.-T. Yau (1993). “Hydrodynamical Limit for a Hamiltonian System with Weak Noise”, *Comm. Math. Phys.* **3**, pp. 523–560.

R. Patterson, S. Simonella, and W. Wagner (2016). “Kinetic theory of cluster dynamics”, *Phys. D: Nonlin. Phen.* **335**, pp. 26–32.

——— (2017). “A Kinetic Equation for the Distribution of Interaction Clusters in Rarefied Gases”, *J. Stat. Phys.* **169** (1), pp. 126–167.

R.E. Peierls (1929). “Zur kinetischen Theorie der Wärmeleitung in Kristallen”, *Annalen Physik* **3**, pp. 1055–1101.

O. Penrose (1967). “Convergence of fugacity expansions for classical systems”, in: *Statistical mechanics: foundations and applications*. A. Bak ed., Benjamin, New York.

S. Poghosyan and D. Ueltschi (2009). “Abstract cluster expansion with applications to statistical mechanical systems”, *J. Math. Phys.* **50** (5), Paper No. 053509, 17 pp.

M. Pulvirenti, C. Saffirio, and S. Simonella (2014). “On the validity of the Boltzmann equation for short range potentials”, *Rev. Math. Phys.* **26** (2), pp. 1–64.

M. Pulvirenti and S. Simonella (2017). “The Boltzmann-Grad limit of a hard sphere system: analysis of the correlation error”, *Invent. Math.* **207** (3), pp. 1135–1237.

——— (2026). “Some Considerations on the Fluid-Dynamical Limit of Particle Systems”, *Mathematics and Mechanics of Complex Systems* **14** (2), pp. 143–154.

C. Qi (2024). *Global Solution of a Functional Hamilton-Jacobi Equation associated with a Hard Sphere Gas*. arXiv: [2409.02805](https://arxiv.org/abs/2409.02805).

D. Ruelle (1969). *Statistical Mechanics. Rigorous Results*. W.A. Benjamin Inc., New York.

S. Simonella and R. Winter (2026). “Pointwise decay of cumulants in chaotic states at low density”, *Markov Processes and Related Fields*. To appear.

H. Spohn (1991). *Large Scale Dynamics of Interacting Particles*. Texts and Monographs in Physics. Springer-Verlag, New York.

——— (1997). “Loschmidt’s Reversibility Argument and the H-Theorem”, *Pioneering Ideas for the Physical and Chemical Sciences*.

A-S. de Suzzoni (2025). “Dérivation de l’équation cinétique associée à l’équation de Schrödinger cubique, d’après Yu Deng et Zaher Hani”, in: *Séminaire Bourbaki. Volume 2023/2024. Exposés 1211–1226*. Astérisque **454**, pp. 341–374.

F. Treves (1970). “An abstract nonlinear Cauchy-Kowalewska theorem”, *Trans. Amer. Math. Soc* **150**, pp. 77–92.

K. Uchiyama (1988). “Derivation of the Boltzmann equation from particle dynamics”, *Hiroshima Math. J.* **18**, pp. 245–297.

S. Ukai (1974). “On the existence of global solutions of mixed problem for non-linear Boltzmann equation”, *Proc. Japan Acad.* **50**, pp. 179–184.

——— (2001). “The Boltzmann-Grad Limit and Cauchy-Kovalevskaya Theorem”, *Japan J. Indust. Appl. Math.* **18**, pp. 383–392.

Thierry Bodineau

I.H.E.S., Université Paris-Saclay, CNRS  
 Laboratoire Alexandre Grothendieck,  
 35 Route de Chartres  
 91440 Bures-sur-Yvette, France  
*E-mail* : [bodineau@ihes.fr](mailto:bodineau@ihes.fr)

Isabelle Gallagher

Université Paris Cité, Sorbonne Université  
 CNRS, IMJ-PRG  
 75013 Paris, France  
*E-mail* : [isabelle.gallagher@u-paris.fr](mailto:isabelle.gallagher@u-paris.fr)

Laure Saint-Raymond

I.H.E.S., Université Paris-Saclay, CNRS  
 Laboratoire Alexandre Grothendieck,  
 35 Route de Chartres  
 91440 Bures-sur-Yvette, France  
*E-mail* : [laure@ihes.fr](mailto:laure@ihes.fr)

Sergio Simonella

Sapienza Università di Roma  
 Dipartimento di Matematica G. Castelnuovo  
 Piazzale A. Moro 5, 00185 Roma, Italy  
*E-mail* : [sergio.simonella@uniroma1.it](mailto:sergio.simonella@uniroma1.it)